Hindawi
Concepts in Magnetic Resonance Part A, Bridging Education and Research
Volume 2022, Article ID 1143341, 18 pages
https://doi.org/10.1155/2022/1143341

*Research Article*

# The Clebsch–Gordan Coefficients and Their Application to Magnetic Resonance

**Edward P. Saliba** [1,2] **and Alexander B. Barnes** [2]

[1]*Francis Bitter Magnet Laboratory, Massachusetts Institute of Technology, Cambridge, MA 02139, USA*
[2]*Laboratory of Physical Chemistry, Eidgenössische Technische Hochschule Zürich, Zürich 8093, Switzerland*

Correspondence should be addressed to Edward P. Saliba; epsaliba@mit.edu

Received 18 September 2021; Accepted 15 December 2021; Published 17 May 2022

Academic Editor: Philippe Lesot



The Clebsch–Gordan coefficients are extremely useful in magnetic resonance theory, yet have an infamous perceived level of complexity by many students. The Clebsch–Gordan coefficients are used to determine both the matrix elements of the spherical tensor operators and the total angular momentum states of a system of component angular momenta. Full derivations of these coefficients are rarely worked through step by step. Instead, students are provided with tables accompanied by little or no explanation of where the values in it originated from. This lack of direction is often a source of confusion for students. For this reason, we work through two common examples of the application of the Clebsch–Gordan coefficients to magnetic resonance experiments. In the first, we determine the components of the magnetic resonance Hamiltonian of ranks 0, 1, and 2 and use these to identify the secular portion of the static, heteronuclear dipolar Hamiltonian. In the second, we derive the singlet and triplet states that arise from the interaction of two identical spin-1/2 particles.

## 1. Introduction

Magnetic resonance experiments play an important role in the study of biology, materials science, and pharmacology, as well as other disciplines [1–16]. In particular, the unparalleled resolution of nuclear magnetic resonance (NMR) spectroscopy makes it ideally suited for the determination of site-specific information about a chemical architecture [5, 7–11]. A rigorous understanding of the theory and spin physics describing magnetic resonance provides not only the ability to interpret experimental data sets but also the insight required to design new experiments.

The Hamiltonian describes the interactions of spins in mathematical form that, along with the density matrix, provides a complete and quantitative framework for magnetic resonance theory. Therefore, the ability to generate an accurate Hamiltonian for the system is of fundamental importance. This includes being able to describe the orientational dependence of anisotropic Hamiltonians, for which the spherical tensor operators are commonly employed [17]. However, much of the literature on the subject takes for granted many aspects of this process, simply stating results rather than showing the origin of the concepts utilized. This has led to a conspicuous hole in the magnetic resonance literature, particularly concerning the Clebsch–Gordan coefficients. The Clebsch–Gordan coefficients play an important role in two different aspects of magnetic resonance calculations. First, they allow for the "second rank tensor components" that are ubiquitously referred to in the literature to be determined from first rank spherical tensors (magnetic field vectors). Additionally, they allow for the total spin states of a system of component angular momenta to be constructed from the component wave functions [18]. In this paper, we provide a detailed strategy for calculating the Clebsch–Gordan coefficients and work through practical examples demonstrating their use.

## 2. The Magnetic Resonance Hamiltonian and Spherical Tensor Operators

One of the most important aspects of performing an accurate spin physics simulation is the ability to generate the

correct Hamiltonian operator with an accurate dependence on molecular orientation. The Hamiltonian is the quantum mechanical operator describing the energy of the system. Classically, the energy of a magnetic moment interacting with a magnetic field is given by equation (1) below [18]:

$$E = -\vec{\mu}^T \vec{B}. \tag{1}$$

In equation (1), $\vec{\mu}$ is the magnetic moment of the spin, the superscript $T$ indicates that we are taking the transpose of this vector, and $\vec{B}$ is the magnetic field vector that the magnetic moment is interacting with.

The way that the quantum mechanical equivalent of equation (1) is commonly written is given by equation (2) below [17]:

$$\hat{H} = \vec{I}^T \overrightarrow{\overrightarrow{A}} \vec{S}. \tag{2}$$

In equation (2), $\vec{I}$ is a vector of the spin operators $\hat{I}_x, \hat{I}_y$, and $\hat{I}_z$. $\vec{S}$ is a general field term that the spin is interacting with and has the components $\hat{S}_x$, $\hat{S}_y$, and $\hat{S}_z$. $\vec{S}$ could be another set of spin operators or the external magnetic field, for example. The relationship between $\vec{I}$ and $\vec{S}$ in equation (2) is qualitatively the same as that between $\vec{\mu}$ and $\vec{B}$ in equation (1). However, equation (2) also contains the additional term $\overrightarrow{\overrightarrow{A}}$. $\overrightarrow{\overrightarrow{A}}$ is a $3 \times 3$ tensor-valued quantity that describes the anisotropic coupling between $\vec{I}$ and $\vec{S}$, showing how the effective size of the magnetic moment changes with the orientation of the molecule in space. It should be noted though that an anisotropic tensor term could also be included in equation (1), but we have chosen to write it as it is commonly found in the literature in its isotropic form. A second important point to consider to avoid confusion is that the spin matrices in $\vec{I}$ do not have any units, unlike $\vec{\mu}$ in equation (1). This discrepancy is made up for by multiplying $\overrightarrow{\overrightarrow{A}}$ by the appropriate constants for the overall Hamiltonian to have units of energy.

Equation (2) can be rewritten in the equivalent and convenient form of equation (3) below [17]:

$$\hat{H} = \mathrm{Tr}\left(\overrightarrow{\overrightarrow{A}} \vec{S} \vec{I}^T\right). \tag{3}$$

In equation (3), the outer product, $\vec{S}\vec{I}^T$, is a $3 \times 3$ matrix, just like $\overrightarrow{\overrightarrow{A}}$. This is shown explicitly in equation (4) below [17]:

$$\begin{aligned} \hat{H} &= \mathrm{Tr}\left[\begin{pmatrix} a_{xx} & a_{xy} & a_{xz} \\ a_{yx} & a_{yy} & a_{yz} \\ a_{zx} & a_{zy} & a_{zz} \end{pmatrix} \begin{pmatrix} \hat{S}_x \\ \hat{S}_y \\ \hat{S}_z \end{pmatrix} \begin{pmatrix} \hat{I}_x & \hat{I}_y & \hat{I}_z \end{pmatrix}\right] \\ &= \mathrm{Tr}\left[\begin{pmatrix} a_{xx} & a_{xy} & a_{xz} \\ a_{yx} & a_{yy} & a_{yz} \\ a_{zx} & a_{zy} & a_{zz} \end{pmatrix} \begin{pmatrix} \hat{S}_x\hat{I}_x & \hat{S}_x\hat{I}_y & \hat{S}_x\hat{I}_z \\ \hat{S}_y\hat{I}_x & \hat{S}_y\hat{I}_y & \hat{S}_y\hat{I}_z \\ \hat{S}_z\hat{I}_x & \hat{S}_z\hat{I}_y & \hat{S}_z\hat{I}_z \end{pmatrix}\right]. \end{aligned} \tag{4}$$

The fact that in equation (4) we have two $3 \times 3$ matrices is convenient, in that they can each be independently expanded into the same orthonormal basis set. The basis set usually chosen is that of the spherical tensors of ranks 0, 1, and 2 because they provide a means to perform a series of many rotations with relatively little effort. These are discussed further in the subsequent sections. The spherical tensor of rank $l$ and $z$-projection $m$ is denoted $\overrightarrow{\overrightarrow{T}}^{(l)}_m$. The orthonormality condition is quantified in equation (5) below, where $\delta_{i,j}$ is the Kronecker delta ($\delta_{i,j} = 1$ if $i = j$, and 0 if $i \neq j$), and the symbol † means to take the conjugate transpose of the matrix [17].

$$\mathrm{Tr}\left[\overrightarrow{\overrightarrow{T}}^{(l)\dagger}_m \overrightarrow{\overrightarrow{T}}^{(l)}_m\right] = \delta_{l_1,l_2}\delta_{m_1,m_2}. \tag{5}$$

The matrix spherical tensors of ranks 0–2 are shown in equations (6a)–(6i) below:

$$\overrightarrow{\overrightarrow{T}}^{(0)}_0 = \begin{pmatrix} -\frac{1}{\sqrt{3}} & 0 & 0 \\ 0 & -\frac{1}{\sqrt{3}} & 0 \\ 0 & 0 & -\frac{1}{\sqrt{3}} \end{pmatrix}, \tag{6a}$$

$$\overrightarrow{\overrightarrow{T}}^{(1)}_1 = \begin{pmatrix} 0 & 0 & \frac{1}{2} \\ 0 & 0 & \frac{i}{2} \\ -\frac{1}{2} & -\frac{i}{2} & 0 \end{pmatrix}, \tag{6b}$$

$$\overrightarrow{\overrightarrow{T}}^{(1)}_0 = \begin{pmatrix} 0 & -\frac{i}{\sqrt{2}} & 0 \\ \frac{i}{\sqrt{2}} & 0 & 0 \\ 0 & 0 & 0 \end{pmatrix}, \tag{6c}$$

$$\overrightarrow{\overrightarrow{T}}^{(1)}_{-1} = \begin{pmatrix} 0 & 0 & \frac{1}{2} \\ 0 & 0 & -\frac{i}{2} \\ -\frac{1}{2} & \frac{i}{2} & 0 \end{pmatrix}, \tag{6d}$$

$$\overrightarrow{\overrightarrow{T}}^{(2)}_2 = \begin{pmatrix} \frac{1}{2} & \frac{i}{2} & 0 \\ \frac{i}{2} & -\frac{1}{2} & 0 \\ 0 & 0 & 0 \end{pmatrix}, \tag{6e}$$

$$\overrightarrow{\overrightarrow{T}}{}^{(2)}_{1} = \begin{pmatrix} 0 & 0 & -\frac{1}{2} \\ 0 & 0 & -\frac{i}{2} \\ -\frac{1}{2} & -\frac{i}{2} & 0 \end{pmatrix}, \tag{6f}$$

$$\overrightarrow{\overrightarrow{T}}{}^{(2)}_{0} = \begin{pmatrix} -\frac{1}{\sqrt{6}} & 0 & 0 \\ 0 & -\frac{1}{\sqrt{6}} & 0 \\ 0 & 0 & \frac{2}{\sqrt{6}} \end{pmatrix}, \tag{6g}$$

$$\overrightarrow{\overrightarrow{T}}{}^{(2)}_{-1} = \begin{pmatrix} 0 & 0 & \frac{1}{2} \\ 0 & 0 & -\frac{i}{2} \\ \frac{1}{2} & -\frac{i}{2} & 0 \end{pmatrix}, \tag{6h}$$

$$\overrightarrow{\overrightarrow{T}}{}^{(2)}_{-2} = \begin{pmatrix} \frac{1}{2} & -\frac{i}{2} & 0 \\ -\frac{i}{2} & -\frac{1}{2} & 0 \\ 0 & 0 & 0 \end{pmatrix}. \tag{6i}$$

From here, the two matrices in equation (4) can each be expanded into the spherical tensor basis and the trace evaluated. This is performed in equation (7) [17]:

$$\begin{aligned} \hat{H} &= \mathrm{Tr}\left[\left(\sum_{l_A=0}^{2}\sum_{m_A=-l_A}^{l_A} a_{m_A}^{(l_A)}\overrightarrow{\overrightarrow{T}}{}^{(l_A)}_{m_A}\right)\left(\sum_{l_s=0}^{2}\sum_{m_s=-l_s}^{l_s} \hat{s}_{m_s}^{(l_s)}\overrightarrow{\overrightarrow{T}}{}^{(l_s)}_{m_s}\right)\right] \\ &= \sum_{l=0}^{2}\sum_{m=-l}^{l} (-1)^m a_m^{(l)}\tilde{s}_{-m}^{(l)}. \end{aligned} \tag{7}$$

The identity $\overrightarrow{\overrightarrow{T}}{}^{(l)}_{m} = (-1)^m \overrightarrow{\overrightarrow{T}}{}^{(l)\dagger}_{-m}$ has been used to obtain the result of equation (7) [17]. The $a_{m_A}^{(l_A)}$'s are the physical space coefficients for their corresponding spherical tensors and are related to the matrix elements of $\overrightarrow{\overrightarrow{A}}$. These are scalar-valued quantities. The $\hat{s}_{m_s}^{(l_s)}$'s are the corresponding spin space coefficients. They are matrix-valued quantities whose dimensions will depend on the number and types of spins present in the spin system. Note that when the trace over the product of the two sums in equation (7) is performed, only the terms with the same value of $l$ and opposite values of $m$ are nonzero due to the orthogonality of the spherical tensor basis. For this reason, we have made the substitutions $l_A = l_s = l$ and $m_A = m_s = m$ in the final equality.

We run into an issue here, however. We are usually supplied with the Cartesian coefficients for the tensor-valued quantities of equation (4), but we are interested in the spherical tensor components. The Clebsch–Gordan coefficients will allow us to determine the spherical components of the matrix spherical tensors of ranks 0, 1, and 2 from the vector spherical tensors of rank 1. They will also allow us to determine the higher rank terms involved in second-order average Hamiltonian theory and above. Furthermore, they can be used to determine the spin states of a system of component angular momenta, in terms of the component wave functions.

## 3. The Clebsch–Gordan Coefficients

*3.1. Definition and Application.* Many discussions of the spherical tensor operators supply the relationships shown in equations (8a)–(8i) below, which relate the Cartesian tensor coefficients with the spherical ones, without elaborating further on their origin [19].

$$a_2^{(2)} = \frac{1}{2}a_{xx} - \frac{1}{2}a_{yy} - \frac{i}{2}a_{xy} - \frac{i}{2}a_{yx}, \tag{8a}$$

$$a_1^{(2)} = -\frac{1}{2}a_{zx} - \frac{1}{2}a_{xz} + \frac{i}{2}a_{zy} + \frac{i}{2}a_{yz}, \tag{8b}$$

$$a_0^{(2)} = \frac{2}{\sqrt{6}}a_{zz} - \frac{1}{\sqrt{6}}a_{xx} - \frac{1}{\sqrt{6}}a_{yy}, \tag{8c}$$

$$a_{-1}^{(2)} = \frac{1}{2}a_{zx} + \frac{1}{2}a_{xz} + \frac{i}{2}a_{zy} + \frac{i}{2}a_{yz}, \tag{8d}$$

$$a_{-2}^{(2)} = \frac{1}{2}a_{xx} - \frac{1}{2}a_{yy} + \frac{i}{2}a_{xy} + \frac{i}{2}a_{yx}, \tag{8e}$$

$$a_1^{(1)} = -\frac{1}{2}a_{zx} + \frac{1}{2}a_{xz} + \frac{i}{2}a_{zy} - \frac{i}{2}a_{yz}, \tag{8f}$$

$$a_0^{(1)} = \frac{i}{\sqrt{2}}a_{xy} - \frac{i}{\sqrt{2}}a_{yx}, \tag{8g}$$

$$a_{-1}^{(1)} = -\frac{1}{2}a_{zx} + \frac{1}{2}a_{xz} - \frac{i}{2}a_{zy} + \frac{i}{2}a_{yz}, \tag{8h}$$

$$a_0^{(0)} = -\frac{1}{\sqrt{3}}a_{xx} - \frac{1}{\sqrt{3}}a_{yy} - \frac{1}{\sqrt{3}}a_{zz}. \tag{8i}$$

The factors in front of the Cartesian coefficients used in equations (8a)–(8i) are related to the Clebsch–Gordan coefficients. Clebsch–Gordan coefficients are commonly

encountered in the study of the addition of quantum angular momenta. In fact, the mathematics of the spherical tensors are isomorphous to that of quantum angular momentum systems.

The Clebsch–Gordan coefficients are usually defined using equation (9) below [18]:

$$\left|j_1, j_2, J, M\right\rangle = \sum_{m_1=-l_1}^{l_1} \sum_{m_2=-l_2}^{l_2} \left(\left\langle j_1, m_1\right| \otimes \left\langle j_2, m_2\right|\right) \left|j_1, j_2, J, M\right\rangle \cdot \left(\left|j_1, m_1\right\rangle \otimes \left|j_2, m_2\right\rangle\right). \tag{9}$$

Here, $j_1$ and $j_2$ are the total angular momentum quantum numbers of two spins, analogous to the ranks of the individual spherical tensor quantities that make up the tensor product of equation (4). The notations $(|j_1, m_1\rangle \otimes |j_2, m_2\rangle)$ and $(\langle j_1, m_1| \otimes \langle j_2, m_2|)$ indicate the ket and bra forms of the product basis of the two-spin system, respectively. $J$ and $M$ are the total rank and $z$-projections for the entire system, respectively. In equation (9), the Clebsch–Gordan coefficients can be extracted as is done in equation (10) below [18]:

$$C_{m_1,m_2,M}^{(j_1,j_2,J)} = \left(\left\langle j_1, m_1\right| \otimes \left\langle j_2, m_2\right|\right) \left|j_1, j_2, J, M\right\rangle. \tag{10}$$

Although the definition of the Clebsch–Gordan coefficients in equation (10) is true, it is not particularly useful for actually determining what their numerical values are. Complicated equations exist to predict what these numbers are, but they are rarely derived in the literature and are quite nonintuitive [20]. In the following section, we present an intuitive method to determine what the Clebsch–Gordan coefficients for a system are.

*3.2. An Intuitive Algorithm to Compute the Clebsch–Gordan Coefficients.* In this section, we describe an intuitive algorithm to generate the Clebsch–Gordan coefficients. We derive the Clebsch–Gordan coefficients for the direct product space of two rank 1 tensors, from which the $3 \times 3$ tensors of ranks 0, 1, and 2 can be determined. Bear in mind that the problem is isomorphous to that of determining the system spin states of two coupled spin-1 particles. The procedure is adapted from that touched on by Griffiths [18] and Shankar [21].

*3.2.1. Determine the Allowed Values of J and M.* The first step in generating the Clebsch–Gordan coefficients is determining which values of $J$ and $M$ are allowed, given the total angular momentum quantum numbers (ranks) of the components of the system ($j_1$ and $j_2$). The rule for the allowed values of $J$ is that it ranges from $|j_1 - j_2|$ to $j_1 + j_2$ in steps of 1. This is concisely written in equation (11) below [18]:

$$\left|j_1 - j_2\right| \leq J \leq j_1 + j_2. \tag{11}$$

This makes sense as the extreme values of possible spin occur when the two spins' z-components are either completely aligned with one another or completely anti-aligned [18]. A complete derivation of the inequalities in equation (11) is provided in Chapter X of the book Quantum Mechanics by Cohen-Tannoudji, Diu, and Laloë [22].

In our example of two rank 1 tensors, $J$ can range from $|1 - 1| = 0$ to $1 + 1 = 2$, in steps of 1, meaning that $J$ can be 0, 1, or 2. From here, the allowed values of $M$ for each $J$ are straightforward to determine, as they range from $-J$ to $J$ in steps of 1, following typical angular momentum rules. An easy way to check to make sure that the correct values are used is that the number of component states used in the algorithm must equal the number of system states obtained. For example, for two rank 1 tensors, there are 9 possible combinations of $m_1$ and $m_2$ (the allowed states are $(|j_1, m_1\rangle \otimes |j_2, m_2\rangle) = (|1, 1\rangle \otimes |1, 1\rangle)$, $(|1, 0\rangle \otimes |1, 1\rangle)$, $(|1, -1\rangle \otimes |1, 1\rangle)$, $(|1, 1\rangle \otimes |1, 0\rangle)$, $(|1, 0\rangle \otimes |1, 0\rangle)$, $(|1, -1\rangle \otimes |1, 0\rangle)$, $(|1, 1\rangle \otimes |1, -1\rangle)$, $(|1, 0\rangle \otimes |1, -1\rangle)$, and $(|1, -1\rangle \otimes |1, -1\rangle)$). Therefore, we should expect 9 states to be output once the Clebsch–Gordan coefficients have been determined. Following the rules we have described, we find that this is, in fact, the case. The allowed states for the total system are $|j_1, j_2, J, M\rangle = |1, 1, 2, 2\rangle$, $|1, 1, 2, 1\rangle$, $|1, 1, 2, 0\rangle$, $|1, 1, 2, -1\rangle$, $|1, 1, 2, -2\rangle$, $|1, 1, 1, 1\rangle$, $|1, 1, 1, 0\rangle$, $|1, 1, 1, -1\rangle$, and $|1, 1, 0, 0\rangle$.

*3.2.2. Determine the Lowering Operators for the Component and System Tensors.* The algorithm for generating the Clebsch–Gordan coefficients that we describe in this section relies on successive applications of lowering operators. The next step is to generate the lowering operators for both the system and for the individual spins that make up the system (note that we have been using the terms "spin" and "rank" interchangeably to reinforce the concept that the mathematics of the spherical tensors is identical to that of a corresponding spin system). This can be accomplished by applying the rules in equations (12a) and (12b) below [23]:

$$\hat{j}_-(j)\left|j, m\right\rangle = \sqrt{j(j+1) - m(m-1)}\left|j, m-1\right\rangle, \tag{12a}$$

$$\hat{j}_{-m,m'}(j) = \left\langle j, m\right|\hat{j}_-(j)\left|j, m'\right\rangle. \tag{12b}$$

Equation (12a) states that the lowering operator for a given spin ($\hat{j}_-(j)$) lowers the state by one $z$-projection quantum number and multiplies it by a factor related to its $j$ and $m$ values. A nice derivation of this result is provided in Chapter 12 of the book Principles of Quantum Mechanics by R. Shankar [21]. Equation (12b) tells how to obtain the $(m, m')$ matrix element of the lowering operator. We provide a brief justification of equation (12b) in Section S9 of the Supplementary Materials. For our example spin system, we are interested in tensors of ranks 0, 1, and 2. It is convenient to create tables that determine what each lowering operator does to each state. The rank 0 tensor has no states to lower, so we omit it. We begin with the rank 1 terms given in Table 1.

The rank 2 case is given in Table 2.

From equation (12b), we can determine the full matrix representation of the lowering operators:

Table 1: The effect of the spin-1 lowering operator on each allowed spin state.

| $j$ | $m$ | $j(j+1)$ | $m(m-1)$ | $j(j+1)-m(m-1)$ | $\sqrt{j(j+1)-m(m-1)}$ |
|---|---|---|---|---|---|
| 1 | 1 | 2 | 0 | 2 | $\sqrt{2}$ |
| 1 | 0 | 2 | 0 | 2 | $\sqrt{2}$ |
| 1 | −1 | 2 | 2 | 0 | 0 |

Table 2: The effect of the spin-2 lowering operator on each allowed spin state.

| $j$ | $m$ | $j(j+1)$ | $m(m-1)$ | $j(j+1)-m(m-1)$ | $\sqrt{j(j+1)-m(m-1)}$ |
|---|---|---|---|---|---|
| 2 | 2 | 6 | 2 | 4 | 2 |
| 2 | 1 | 6 | 0 | 6 | $\sqrt{6}$ |
| 2 | 0 | 6 | 0 | 6 | $\sqrt{6}$ |
| 2 | −1 | 6 | 2 | 4 | 2 |
| 2 | −2 | 6 | 6 | 0 | 0 |

$$\widehat{j}_{-}(1)=\begin{pmatrix} \langle 1,1|\widehat{j}_{-}(1)|1,1\rangle & \langle 1,1|\widehat{j}_{-}(1)|1,0\rangle & \langle 1,1|\widehat{j}_{-}(1)|1,-1\rangle \\ \langle 1,0|\widehat{j}_{-}(1)|1,1\rangle & \langle 1,0|\widehat{j}_{-}(1)|1,0\rangle & \langle 1,0|\widehat{j}_{-}(1)|1,-1\rangle \\ \langle 1,-1|\widehat{j}_{-}(1)|1,1\rangle & \langle 1,-1|\widehat{j}_{-}(1)|1,0\rangle & \langle 1,-1|\widehat{j}_{-}(1)|1,-1\rangle \end{pmatrix}, \tag{13a}$$

$$\widehat{j}_{-}(2)=\begin{pmatrix} \langle 2,2|\widehat{j}_{-}(2)|2,2\rangle & \langle 2,2|\widehat{j}_{-}(2)|2,1\rangle & \langle 2,2|\widehat{j}_{-}(2)|2,0\rangle & \langle 2,2|\widehat{j}_{-}(2)|2,-1\rangle & \langle 2,2|\widehat{j}_{-}(2)|2,-2\rangle \\ \langle 2,1|\widehat{j}_{-}(2)|2,2\rangle & \langle 2,1|\widehat{j}_{-}(2)|2,1\rangle & \langle 2,1|\widehat{j}_{-}(2)|2,0\rangle & \langle 2,1|\widehat{j}_{-}(2)|2,-1\rangle & \langle 1,1|\widehat{j}_{-}(2)|2,-2\rangle \\ \langle 2,0|\widehat{j}_{-}(2)|2,2\rangle & \langle 2,0|\widehat{j}_{-}(2)|2,1\rangle & \langle 2,0|\widehat{j}_{-}(2)|2,0\rangle & \langle 2,0|\widehat{j}_{-}(2)|2,-1\rangle & \langle 2,0|\widehat{j}_{-}(2)|2,-2\rangle \\ \langle 2,-1|\widehat{j}_{-}(2)|2,2\rangle & \langle 2,-1|\widehat{j}_{-}(2)|2,1\rangle & \langle 2,-1|\widehat{j}_{-}(2)|2,0\rangle & \langle 2,-1|\widehat{j}_{-}(2)|2,-1\rangle & \langle 2,-1|\widehat{j}_{-}(2)|2,-2\rangle \\ \langle 2,-2|\widehat{j}_{-}(2)|2,2\rangle & \langle 2,-2|\widehat{j}_{-}(2)|2,1\rangle & \langle 2,-2|\widehat{j}_{-}(2)|2,0\rangle & \langle 2,-2|\widehat{j}_{-}(2)|2,-1\rangle & \langle 2,-2|\widehat{j}_{-}(2)|2,-2\rangle \end{pmatrix}. \tag{13b}$$

Applying the rule in equation (12a) then allows equations (13a) and (13b) to be evaluated. This is done in equations (14a) and (14b) below. We have also used the rule $\widehat{j}_{-}(j)|j,-j\rangle=\overrightarrow{0}$ (the lowest allowed $z$-projection cannot be lowered any further):

$$\widehat{j}_{-}(1)=\begin{pmatrix} \sqrt{2}\langle 1,1|1,0\rangle & \sqrt{2}\langle 1,1|1,-1\rangle & 0 \\ \sqrt{2}\langle 1,0|1,0\rangle & \sqrt{2}\langle 1,0|1,-1\rangle & 0 \\ \sqrt{2}\langle 1,-1|1,0\rangle & \sqrt{2}\langle 1,-1|1,-1\rangle & 0 \end{pmatrix}, \tag{14a}$$

$$\widehat{j}_{-}(2)=\begin{pmatrix} 2\langle 2,2|2,1\rangle & \sqrt{6}\langle 2,2|2,0\rangle & \sqrt{6}\langle 2,2|2,-1\rangle & 2\langle 2,2|2,-2\rangle & 0 \\ 2\langle 2,1|2,1\rangle & \sqrt{6}\langle 2,1|2,0\rangle & \sqrt{6}\langle 2,1|2,-1\rangle & 2\langle 2,1|2,-2\rangle & 0 \\ 2\langle 2,0|2,1\rangle & \sqrt{6}\langle 2,0|2,0\rangle & \sqrt{6}\langle 2,0|2,-1\rangle & 2\langle 2,0|2,-2\rangle & 0 \\ 2\langle 2,-1|2,1\rangle & \sqrt{6}\langle 2,-1|2,0\rangle & \sqrt{6}\langle 2,-1|2,-1\rangle & 2\langle 2,-1|2,-2\rangle & 0 \\ 2\langle 2,-2|2,1\rangle & \sqrt{6}\langle 2,-2|2,0\rangle & \sqrt{6}\langle 2,-2|2,-1\rangle & 2\langle 2,-2|2,-2\rangle & 0 \end{pmatrix}. \tag{14b}$$

From here, orthonormality of the basis states can be used to evaluate the matrix elements, with $\langle i|j\rangle=\delta_{i,j}$. This is performed in equations (15a) and (15b) below:

$$\hat{j}_-(1) = \begin{pmatrix} 0 & 0 & 0 \\ \sqrt{2} & 0 & 0 \\ 0 & \sqrt{2} & 0 \end{pmatrix}, \tag{15a}$$

$$\hat{j}_-(2) = \begin{pmatrix} 0 & 0 & 0 & 0 & 0 \\ 2 & 0 & 0 & 0 & 0 \\ 0 & \sqrt{6} & 0 & 0 & 0 \\ 0 & 0 & \sqrt{6} & 0 & 0 \\ 0 & 0 & 0 & 2 & 0 \end{pmatrix}. \tag{15b}$$

These are the lowering operators for rank 1 and rank 2 tensors. They will be used in the following section.

*3.2.3. Write the System Spin States as Linear Combinations of the Component Spin States.* We now want to write the system spin states in terms of the component spin states. The resulting weights of the linear combination are the Clebsch–Gordan coefficients. In order to begin this process, there are a couple of useful rules to keep in mind. First, $C^{(j_1,j_2,J)}_{m_1,m_2,M}$ is only nonzero if $m_1 + m_2 = M$ [18]. Another useful rule is given by equation (16), where the left side of the equation is the total angular momentum state and the right side is the linear combination of component states:

$$\left|j_1, j_2, j_1 + j_2, j_1 + j_2\right\rangle = 1\left(\left|j_1, j_1\right\rangle \otimes \left|j_2, j_2\right\rangle\right). \tag{16}$$

This says that the highest $z$-projection of the highest allowed system spin is equal to the component state with both component spins in their highest $z$-projection state. We have explicitly written the "1" in front of the component state to emphasize that this is the only nonzero Clebsch–Gordan coefficient for the $|j_1, j_2, j_1 + j_2, j_1 + j_2\rangle$ state. The fact that equation (16) is true makes sense, as this is the only state for which $m_1 + m_2 = j_1 + j_2$. In our example of two rank 1 vector spherical tensors, this gives equation (17) below:

$$|1,1,2,2\rangle = 1\,(|1,1\rangle \otimes |1,1\rangle). \tag{17}$$

From here, we can simply use successive applications of the total lowering operator (which is the sum of the individual lowering operators) to solve for the other rank 2 terms. Note that we are interested in the rank 2 terms at the moment, so we know that the system lowering operator must act on the rank 2 states like a spin-2 lowering operator. For this reason, we use the notation $\hat{J}_-(2)$ to indicate the total lowering operator for the system. The first round of this process is carried through equations (18a)–(18c) below. Note that the Clebsch–Gordan coefficents are the numbers in front of the component spin states in the last line of the derivation (equation (18c)):

$$\hat{J}_-(2)|1,1,2,2\rangle = \left(\hat{j}_-^{(1)}(1) + \hat{j}_-^{(2)}(1)\right)(|1,1\rangle \otimes |1,1\rangle), \tag{18a}$$

$$2|1,1,2,1\rangle = \sqrt{2}\,(|1,0\rangle \otimes |1,1\rangle) + \sqrt{2}\,(|1,1\rangle \otimes |1,0\rangle), \tag{18b}$$

$$\begin{aligned} |1,1,2,1\rangle &= \frac{\sqrt{2}}{2}\,(|1,0\rangle \otimes |1,1\rangle) + \frac{\sqrt{2}}{2}\,(|1,1\rangle \otimes |1,0\rangle) \\ &= \frac{1}{\sqrt{2}}\,(|1,0\rangle \otimes |1,1\rangle) + \frac{1}{\sqrt{2}}\,(|1,1\rangle \otimes |1,0\rangle). \end{aligned} \tag{18c}$$

In equation (18a), $\hat{J}_-(2)$ is the rank 2 lowering operator for the system, and $\hat{j}_-^{(1)}(1)$ and $\hat{j}_-^{(2)}(1)$ are the rank 1 lowering operators for the component spins 1 and 2, respectively. Note that $\hat{j}_-^{(1)}(1)$ only affects spin number 1 and $\hat{j}_-^{(2)}(1)$ only affects spin number 2. From here, the lowering operator can again be applied. This is carried through in equations (19a)–(19d) below:

$$\hat{J}_-(2)|1,1,2,1\rangle = \left(\hat{j}_-^{(1)}(1) + \hat{j}_-^{(2)}(1)\right)\left(\frac{1}{\sqrt{2}}\,(|1,0\rangle \otimes |1,1\rangle) + \frac{1}{\sqrt{2}}\,(|1,1\rangle \otimes |1,0\rangle)\right), \tag{19a}$$

$$\begin{aligned} \sqrt{6}|1,1,2,0\rangle = {} & \sqrt{2}\left(\frac{1}{\sqrt{2}}\right)(|1,-1\rangle \otimes |1,1\rangle) + \sqrt{2}\left(\frac{1}{\sqrt{2}}\right)(|1,0\rangle \otimes |1,0\rangle) \\ & + \sqrt{2}\left(\frac{1}{\sqrt{2}}\right)(|1,0\rangle \otimes |1,0\rangle) + \sqrt{2}\left(\frac{1}{\sqrt{2}}\right)(|1,1\rangle \otimes |1,-1\rangle), \end{aligned} \tag{19b}$$

$$\sqrt{6}|1,1,2,0\rangle = (|1,-1\rangle \otimes |1,1\rangle) + 2\,(|1,0\rangle \otimes |1,0\rangle) + (|1,1\rangle \otimes |1,-1\rangle), \tag{19c}$$

$$|1,1,2,0\rangle = \frac{1}{\sqrt{6}}\,(|1,-1\rangle \otimes |1,1\rangle) + \frac{2}{\sqrt{6}}\,(|1,0\rangle \otimes |1,0\rangle) + \frac{1}{\sqrt{6}}\,(|1,1\rangle \otimes |1,-1\rangle). \tag{19d}$$

This process can now be continued for the other $J = 2$ states, as is done in equations (20a)–(21d). In cases where the lowering operator is applied to the lowest possible spin state, resulting in the zero vector, we have omitted the calculation. Once again, note that the Clebsch–Gordan coefficients are the numbers appearing before each of the component states on the right side of the final line in each derivation (equations (20e) and (21d)):

$$\hat{J}_-(2)|1,1,2,0\rangle = \left(\hat{j}_-^{(1)}(1) + \hat{j}_-^{(2)}(1)\right) \times\left(\frac{1}{\sqrt{6}}\left(|1,-1\right\rangle \otimes |1,1\rangle) + \frac{2}{\sqrt{6}}\left(|1,0\rangle \otimes |1,0\rangle\right) + \frac{1}{\sqrt{6}}\left(|1,1\rangle \otimes |1,-1\rangle\right)\right), \tag{20a}$$

$$\sqrt{6}|1,1,2,-1\rangle = \sqrt{2}\left(\frac{2}{\sqrt{6}}\right)(|1,-1\rangle \otimes |1,0\rangle) + \sqrt{2}\left(\frac{1}{\sqrt{6}}\right)(|1,0\rangle \otimes |1,-1\rangle) + \sqrt{2}\left(\frac{1}{\sqrt{6}}\right)(|1,-1\rangle \otimes |1,0\rangle) + \sqrt{2}\left(\frac{2}{\sqrt{6}}\right)(|1,0\rangle \otimes |1,-1\rangle), \tag{20b}$$

$$\sqrt{6}|1,1,2,-1\rangle = \sqrt{3}\,(|1,-1\rangle \otimes |1,0\rangle) + \sqrt{3}\,(|1,0\rangle \otimes |1,-1\rangle), \tag{20c}$$

$$|1,1,2,-1\rangle = \frac{\sqrt{3}}{\sqrt{6}}\,(|1,-1\rangle \otimes |1,0\rangle) + \frac{\sqrt{3}}{\sqrt{6}}\,(|1,0\rangle \otimes |1,-1\rangle), \tag{20d}$$

$$|1,1,2,-1\rangle = \frac{1}{\sqrt{2}}\,(|1,-1\rangle \otimes |1,0\rangle) + \frac{1}{\sqrt{2}}\,(|1,0\rangle \otimes |1,-1\rangle), \tag{20e}$$

$$\hat{J}_-(2)|1,1,2,-1\rangle = \left(\hat{j}_-^{(1)}(1) + \hat{j}_-^{(2)}(1)\right)\left(\frac{1}{\sqrt{2}}\left(|1,-1\right\rangle \otimes |1,0\rangle) + \frac{1}{\sqrt{2}}\left(|1,0\rangle \otimes |1,-1\rangle\right)\right), \tag{21a}$$

$$2|1,1,2,-2\rangle = \sqrt{2}\left(\frac{1}{\sqrt{2}}\right)(|1,-1\rangle \otimes |1,-1\rangle) + \sqrt{2}\left(\frac{1}{\sqrt{2}}\right)(|1,-1\rangle \otimes |1,-1\rangle), \tag{21b}$$

$$2|1,1,2,-2\rangle = 2\,(|1,-1\rangle \otimes |1,-1\rangle), \tag{21c}$$

$$|1,1,2,-2\rangle = 1\,(|1,-1\rangle \otimes |1,-1\rangle). \tag{21d}$$

This completes the determination of the $J = 2$ states for a system of two spin-1 spins. The resulting linear combinations of component states are summarized in quations (22a)-(22b) below. Again, the Clebsch–Gordon coefficients are the coeffcients in front of the component states on the right-hand side of each of these equations:

$$|1,1,2,2\rangle = 1\,(|1,1\rangle \otimes |1,1\rangle), \tag{22a}$$

$$|1,1,2,1\rangle = \frac{1}{\sqrt{2}}\,(|1,0\rangle \otimes |1,1\rangle) + \frac{1}{\sqrt{2}}\,(|1,1\rangle \otimes |1,0\rangle), \tag{22b}$$

$$|1,1,2,0\rangle = \frac{1}{\sqrt{6}}\,(|1,-1\rangle \otimes |1,1\rangle) + \frac{2}{\sqrt{6}}\,(|1,0\rangle \otimes |1,0\rangle) + \frac{1}{\sqrt{6}}\,(|1,1\rangle \otimes |1,-1\rangle), \tag{22c}$$

$$|1,1,2,-1\rangle = \frac{1}{\sqrt{2}}\,(|1,0\rangle \otimes |1,-1\rangle) + \frac{1}{\sqrt{2}}\,(|1,-1\rangle \otimes |1,0\rangle), \tag{22d}$$

$$|1,1,2,-2\rangle = 1\,(|1,-1\rangle \otimes |1,-1\rangle). \tag{22e}$$

The $J = 2$ case gives 5 system states. However, there are 9 component states. Therefore, we need to produce 4 more states. These will arise from the three $J = 1$ states and one $J = 0$ state. We can now generate the $J = 1$ states. However, we need to start with the state $|j_1, j_2, J, M\rangle = |1,1,1,1\rangle$, but we already have an $M = 1$ state that corresponds to $J = 2$. We can obtain an acceptable state with $J = 1$ and $M = 1$ by demanding that $\langle 1,1,2,1|t1,1,1,1\rangle = 0$. This is done in equations (23a)–(23f). In equations (23d)–(23f), we have used the fact that the sum of the squares of the coefficients for the linear combination must be 1 in order to maintain the normalization of the wave function. Furthermore, it should

be noted that the Clebsch–Gordan coefficients are only unique up to a complex phase factor. We have chosen this phase factor to conform to the Condon–Shortley phase convention and Wigner sign convention described by Baird and Biedenharn [24]. These are standard conventions and match those used by Mathematica, for example [25]. Another advantage of this convention is that all of the Clebsch–Gordan coefficients work out to be real numbers when it is used [24]. Conveniently, this is also the phase convention that occurs naturally with no modification when adhering the algorithm described herein:

$$\begin{aligned}\langle 1,1,2,1|1,1,1,1\rangle = &\left(\frac{1}{\sqrt{2}}\left(\langle 1,0|\otimes\langle 1,1|\right)+\frac{1}{\sqrt{2}}\left(\langle 1,1|\langle|\otimes|\langle 1,0|\right)\right)\\ &\times\left(C_{0,1,1}^{(1,1,1)}\left(|1,0\rangle\otimes|1,1\rangle\right)+C_{1,0,1}^{(1,1,1)}\left(|1,1\rangle\otimes|1,0\rangle\right)\right),\end{aligned} \tag{23a}$$

$$0=\frac{1}{\sqrt{2}}C_{0,1,1}^{(1,1,1)}+\frac{1}{\sqrt{2}}C_{1,0,1}^{(1,1,1)}, \tag{23b}$$

$$C_{0,1,1}^{(1,1,1)}=-C_{1,0,1}^{(1,1,1)}, \tag{23c}$$

$$C_{1,0,1}^{(1,1,1)}=\frac{1}{\sqrt{2}}, \tag{23d}$$

$$C_{0,1,1}^{(1,1,1)}=-\frac{1}{\sqrt{2}}, \tag{23e}$$

$$|1,1,1,1\rangle=-\frac{1}{\sqrt{2}}\left(|1,0\rangle\otimes|1,1\rangle\right)+\frac{1}{\sqrt{2}}\left(|1,1\rangle\otimes|1,0\rangle\right). \tag{23f}$$

From here, we can proceed in much the same manner as before by applying the (now spin-1) lowering operator successively until all of the spin-1 system states have been determined. In this case, we use the notation $\hat{J}_-(1)$, as we now need it to behave like a spin-1 lowering operator when applied to the total state of the system. This is performed in equations (24a)–(25d) below:

$$\hat{J}_-(1)|1,1,1,1\rangle=\left(\hat{j}_-^{(1)}(1)+\hat{j}_-^{(2)}(1)\right)\left(-\frac{1}{\sqrt{2}}\left(|1,0\rangle\otimes|1,1\rangle\right)+\frac{1}{\sqrt{2}}\left(|1,1\rangle\otimes|1,0\rangle\right)\right), \tag{24a}$$

$$\begin{aligned}\sqrt{2}|1,1,1,0\rangle = &-\sqrt{2}\left(\frac{1}{\sqrt{2}}\right)\left(|1,-1\rangle\otimes|1,1\rangle\right)+\sqrt{2}\left(\frac{1}{\sqrt{2}}\right)\left(|1,0\rangle\otimes|1,0\rangle\right)\\ &-\sqrt{2}\left(\frac{1}{\sqrt{2}}\right)\left(|1,0\rangle\otimes|1,0\rangle\right)+\sqrt{2}\left(\frac{1}{\sqrt{2}}\right)\left(|1,1\rangle\otimes|1,-1\rangle\right),\end{aligned} \tag{24b}$$

$$\sqrt{2}|1,1,1,0\rangle=-\left(|1,-1\rangle\otimes|1,1\rangle\right)+\left(|1,1\rangle\otimes|1,-1\rangle\right), \tag{24c}$$

$$|1,1,1,0\rangle=-\frac{1}{\sqrt{2}}\left(|1,-1\rangle\otimes|1,1\rangle\right)+\frac{1}{\sqrt{2}}\left(|1,1\rangle\otimes|1,-1\rangle\right), \tag{24d}$$

$$\hat{J}_-(1)|1,1,1,0\rangle=\left(\hat{j}_-^{(1)}(1)+\hat{j}_-^{(2)}(1)\right)\left(-\frac{1}{\sqrt{2}}\left(|1,-1\rangle\otimes|1,1\rangle\right)+\frac{1}{\sqrt{2}}\left(|1,1\rangle\otimes|1,-1\rangle\right)\right), \tag{25a}$$

$$\sqrt{2}|1,1,1,-1\rangle=\sqrt{2}\left(\frac{1}{\sqrt{2}}\right)\left(|1,0\rangle\otimes|1,-1\rangle\right)-\sqrt{2}\left(\frac{1}{\sqrt{2}}\right)\left(|1,-1\rangle\otimes|1,0\rangle\right), \tag{25b}$$

$$\sqrt{2}|1,1,1,-1\rangle=\left(|1,0\rangle\otimes|1,-1\rangle\right)-\left(|1,-1\rangle\otimes|1,0\rangle\right), \tag{25c}$$

$$|1,1,1,-1\rangle = \frac{1}{\sqrt{2}}(|1,0\rangle \otimes |1,-1\rangle) - \frac{1}{\sqrt{2}}(|1,-1\rangle \otimes |1,0\rangle), \tag{25d}$$

The $J = 1$ states are summarized in equations (26a)–(26c), with the Clebsch–Gordan coefficients being the numbers in front of each of the component states on the right-hand side of each equation:

$$|1,1,1,1\rangle = -\frac{1}{\sqrt{2}}(|1,0\rangle \otimes |1,1\rangle) + \frac{1}{\sqrt{2}}(|1,1\rangle \otimes |1,0\rangle), \tag{26a}$$

$$|1,1,1,0\rangle = -\frac{1}{\sqrt{2}}(|1,-1\rangle \otimes |1,1\rangle) + \frac{1}{\sqrt{2}}(|1,1\rangle \otimes |1,-1\rangle), \tag{26b}$$

$$|1,1,1,-1\rangle = \frac{1}{\sqrt{2}}(|1,0\rangle \otimes |1,-1\rangle) - \frac{1}{\sqrt{2}}(|1,-1\rangle \otimes |1,0\rangle). \tag{26c}$$

We now have 8 states and their corresponding Clebsch–Gordan coefficients (5 from $J = 2$, and 3 from $J = 1$). We finally need the Clebsch–Gordan coefficients for the state $|j_1, j_2, J, M\rangle = |1,1,0,0\rangle$. In order to accomplish this, we proceed in much the same way that we used to solve for the $|1,1,1,1\rangle$ state; only now, it needs to be orthogonal to both $|j_1, j_2, J, M\rangle = |1,1,2,0\rangle$ and $|j_1, j_2, J, M\rangle = |1,1,1,0\rangle$ states. This gives the simultaneous system of equations (27a) and (27b) below:

$$\begin{aligned}\langle 1,1,2,0|1,1,0,0\rangle = 0 = \Bigg(&\frac{1}{\sqrt{6}}\Big(\Big\langle 1,-1| \otimes \Big\langle 1,1| + \frac{2}{\sqrt{6}}\Big(\Big\langle 1,0| \otimes \Big\langle 1,0| + \frac{1}{\sqrt{6}}(\langle 1,1| \otimes \langle 1,-1|)\Big)\\ &\times\Big(C^{(1,1,0)}_{-1,1,0}(|1,-1\rangle \otimes |1,1\rangle) + C^{(1,1,0)}_{0,0,0}(|1,0\rangle \otimes |1,0\rangle) + C^{(1,1,0)}_{1,-1,0}(|1,1\rangle \otimes |1,-1\rangle)\Big),\end{aligned} \tag{27a}$$

$$\begin{aligned}\langle 1,1,1,0|1,1,0,0\rangle = 0 = \Bigg(&-\frac{1}{\sqrt{2}}\Big(\Big\langle 1,-1| \otimes \Big\langle 1,1| + \frac{1}{\sqrt{2}}(\langle 1,1| \otimes \langle 1,-1|)\Big)\\ &\times\Big(C^{(1,1,0)}_{-1,1,0}(|1,-1\rangle \otimes |1,1\rangle) + C^{(1,1,0)}_{0,0,0}(|1,0\rangle \otimes |1,0\rangle) + C^{(1,1,0)}_{1,-1,0}(|1,1\rangle \otimes |1,-1\rangle)\Big).\end{aligned} \tag{27b}$$

This leads to the following derivation in equations (28a)–(28i):

$$0 = \frac{1}{\sqrt{6}}C^{(1,1,0)}_{-1,1,0} + \frac{2}{\sqrt{6}}C^{(1,1,0)}_{0,0,0} + \frac{1}{\sqrt{6}}C^{(1,1,0)}_{1,-1,0}, \tag{28a}$$

$$0 = -\frac{1}{\sqrt{2}}C^{(1,1,0)}_{-1,1,0} + \frac{1}{\sqrt{2}}C^{(1,1,0)}_{1,-1,0}, \tag{28b}$$

$$C^{(1,1,0)}_{1,-1,0} = C^{(1,1,0)}_{-1,1,0}, \tag{28c}$$

$$0 = \frac{1}{\sqrt{6}}C^{(1,1,0)}_{-1,1,0} + \frac{2}{\sqrt{6}}C^{(1,1,0)}_{0,0,0} + \frac{1}{\sqrt{6}}C^{(1,1,0)}_{-1,1,0}, \tag{28d}$$

$$C^{(1,1,0)}_{0,0,0} = -C^{(1,1,0)}_{-1,1,0}, \tag{28e}$$

$$C^{(1,1,0)}_{-1,1,0} = \frac{1}{\sqrt{3}}, \tag{28f}$$

$$C^{(1,1,0)}_{1,-1,0} = \frac{1}{\sqrt{3}}, \tag{28g}$$

$$C^{(1,1,0)}_{0,0,0} = -\frac{1}{\sqrt{3}}, \tag{28h}$$

$$|1,1,0,0\rangle = \frac{1}{\sqrt{3}}(|1,-1\rangle \otimes |1,1\rangle) - \frac{1}{\sqrt{3}}(|1,0\rangle \otimes |1,0\rangle) + \frac{1}{\sqrt{3}}(|1,1\rangle \otimes |1,-1\rangle). \tag{28i}$$

Again, the overall phase of the wave function has been chosen to use the Condon-Shortley phase convention that is used by Mathematica, and they have been chosen to produce a normalized wave function. To summarize, all 9 system states are reproduced in equations (29a)–(29i) below:

$$|1,1,2,2\rangle = 1(|1,1\rangle \otimes |1,1\rangle), \tag{29a}$$

$$|1,1,2,1\rangle = \frac{1}{\sqrt{2}}(|1,0\rangle \otimes |1,1\rangle) + \frac{1}{\sqrt{2}}(|1,1\rangle \otimes |1,0\rangle), \tag{29b}$$

$$|1,1,2,0\rangle = \frac{1}{\sqrt{6}}(|1,-1\rangle \otimes |1,1\rangle) + \frac{2}{\sqrt{6}}(|1,0\rangle \otimes |1,0\rangle) + \frac{1}{\sqrt{6}}(|1,1\rangle \otimes |1,-1\rangle), \tag{29c}$$

$$|1,1,2,-1\rangle = \frac{1}{\sqrt{2}}(|1,0\rangle \otimes |1,-1\rangle) + \frac{1}{\sqrt{2}}(|1,-1\rangle \otimes |1,0\rangle), \tag{29d}$$

$$|1,1,2,-2\rangle = 1(|1,-1\rangle \otimes |1,-1\rangle), \tag{29e}$$

$$|1,1,1,1\rangle = -\frac{1}{\sqrt{2}}(|1,0\rangle \otimes |1,1\rangle) + \frac{1}{\sqrt{2}}(|1,1\rangle \otimes |1,0\rangle), \tag{29f}$$

$$|1,1,1,0\rangle = -\frac{1}{\sqrt{2}}(|1,-1\rangle \otimes |1,1\rangle) + \frac{1}{\sqrt{2}}(|1,1\rangle \otimes |1,-1\rangle), \tag{29g}$$

$$|1,1,1,-1\rangle = \frac{1}{\sqrt{2}}(|1,0\rangle \otimes |1,-1\rangle) - \frac{1}{\sqrt{2}}(|1,-1\rangle \otimes |1,0\rangle), \tag{29h}$$

$$|1,1,0,0\rangle = \frac{1}{\sqrt{3}}(|1,-1\rangle \otimes |1,1\rangle) - \frac{1}{\sqrt{3}}(|1,0\rangle \otimes |1,0\rangle) + \frac{1}{\sqrt{3}}(|1,1\rangle \otimes |1,-1\rangle). \tag{29i}$$

Although the example used here involved 2 spins of spin-1, this same procedure can be used for any two spins (or the equivalent calculation for tensor-valued quantities). All of these can be verified using Mathematica's "ClebschGordan $[\{j_1, m_1\},\{j_2, m_2\},\{J, M\}]$" command.

## 4. The Clebsch–Gordan Coefficients and Spherical Tensors

The spherical tensors are tensors which rotate according to equation (30) below [17]:

$$\overrightarrow{\overrightarrow{T}}^{(l)}_{m}(\text{new frame}) = \sum_{m'=-l}^{l} D^{(l)}_{m',m}\, \overrightarrow{\overrightarrow{T}}^{(l)}_{m'}(\text{old frame}). \tag{30}$$

Here, the $D^{(l)}_{m,m'}$'s are the matrix elements of the Wigner rotation matrix. As we have stated previously and will continue to stress throughout this text, the rotational behavior of the spherical tensor operators is identical to that of the corresponding spin states of the same values of $l$ and $m$. Further explanation of this relationship is provided by Shankar [21]. For vectors, which are tensors of rank 1, the basis elements that have this property are given by in equations (31a)–(31c) below:

$$\overrightarrow{T}^{(1)}_{1} = \begin{pmatrix} -\frac{1}{\sqrt{2}} \\ -\frac{i}{\sqrt{2}} \\ 0 \end{pmatrix}, \tag{31a}$$

$$\overrightarrow{T}^{(1)}_{0} = \begin{pmatrix} 0 \\ 0 \\ 1 \end{pmatrix}, \tag{31b}$$

$$\overrightarrow{T}^{(1)}_{-1} = \begin{pmatrix} \frac{1}{\sqrt{2}} \\ -\frac{i}{\sqrt{2}} \\ 0 \end{pmatrix}. \tag{31c}$$

The importance of the Clebsch–Gordan coefficients to the spherical tensor operators can be realized by first considering the behavior of the Cartesian basis vectors given by equations (32a)–(32c) below:

$$\overrightarrow{i} = \begin{pmatrix} 1 \\ 0 \\ 0 \end{pmatrix}, \tag{32a}$$

$$\overrightarrow{j} = \begin{pmatrix} 0 \\ 1 \\ 0 \end{pmatrix}, \tag{32b}$$

$$\overrightarrow{k} = \begin{pmatrix} 0 \\ 0 \\ 1 \end{pmatrix}. \tag{32c}$$

In order to obtain terms describing the interactions of a spin with other fields, we need to take outer products of these vectors with themselves. If this is done with the Cartesian

vectors, we obtain the following 9 matrices (equations (33a)–(33i)):

$$\vec{i}\,\vec{i}^{T} = \begin{pmatrix} 1 & 0 & 0 \\ 0 & 0 & 0 \\ 0 & 0 & 0 \end{pmatrix}, \tag{33a}$$

$$\vec{i}\,\vec{j}^{T} = \begin{pmatrix} 0 & 1 & 0 \\ 0 & 0 & 0 \\ 0 & 0 & 0 \end{pmatrix}, \tag{33b}$$

$$\vec{i}\,\vec{k}^{T} = \begin{pmatrix} 0 & 0 & 1 \\ 0 & 0 & 0 \\ 0 & 0 & 0 \end{pmatrix}, \tag{33c}$$

$$\vec{j}\,\vec{i}^{T} = \begin{pmatrix} 0 & 0 & 0 \\ 1 & 0 & 0 \\ 0 & 0 & 0 \end{pmatrix}, \tag{33d}$$

$$\vec{j}\,\vec{j}^{T} = \begin{pmatrix} 0 & 0 & 0 \\ 0 & 1 & 0 \\ 0 & 0 & 0 \end{pmatrix}, \tag{33e}$$

$$\vec{j}\,\vec{k}^{T} = \begin{pmatrix} 0 & 0 & 0 \\ 0 & 0 & 1 \\ 0 & 0 & 0 \end{pmatrix}, \tag{33f}$$

$$\vec{k}\,\vec{i}^{T} = \begin{pmatrix} 0 & 0 & 0 \\ 0 & 0 & 0 \\ 1 & 0 & 0 \end{pmatrix}, \tag{33g}$$

$$\vec{k}\,\vec{j}^{T} = \begin{pmatrix} 0 & 0 & 0 \\ 0 & 0 & 0 \\ 0 & 1 & 0 \end{pmatrix}, \tag{33h}$$

$$\vec{k}\,\vec{k}^{T} = \begin{pmatrix} 0 & 0 & 0 \\ 0 & 0 & 0 \\ 0 & 0 & 1 \end{pmatrix}. \tag{33i}$$

From equations (33a)–(33i), we see that if the outer product of two Cartesian basis vectors is calculated, a Cartesian basis tensor is the result. This is not the case for the spherical basis: the outer product of two spherical vectors does not necessarily produce a spherical tensor with the correct rotational property given by equation (30). The Clebsch–Gordan coefficients, however, provide us with the coefficients necessary to construct spherical tensors from linear combinations of the outer products of spherical vectors. They can be constructed in a completely analogous way to the strategy we used to build up the system wave functions from component wave functions in the previous section. Thus, we obtain the following 9 relationships of equations (34a)–(34i):

$$\vec{\vec{T}}^{(2)}_{2} = 1\,\vec{T}^{(1)}_{1}\vec{T}^{(1)T}_{1}, \tag{34a}$$

$$\vec{\vec{T}}^{(2)}_{1} = \frac{1}{\sqrt{2}}\vec{T}^{(1)}_{0}\vec{T}^{(1)T}_{1} + \frac{1}{\sqrt{2}}\vec{T}^{(1)}_{1}\vec{T}^{(1)T}_{0}, \tag{34b}$$

$$\vec{\vec{T}}^{(2)}_{0} = \frac{1}{\sqrt{6}}\vec{T}^{(1)}_{-1}\vec{T}^{(1)T}_{1} + \frac{2}{\sqrt{6}}\vec{T}^{(1)}_{0}\vec{T}^{(1)T}_{0} + \frac{1}{\sqrt{6}}\vec{T}^{(1)}_{1}\vec{T}^{(1)T}_{-1}, \tag{34c}$$

$$\vec{\vec{T}}^{(2)}_{-1} = \frac{1}{\sqrt{2}}\vec{T}^{(1)}_{0}\vec{T}^{(1)T}_{-1} + \frac{1}{\sqrt{2}}\vec{T}^{(1)}_{-1}\vec{T}^{(1)T}_{0}, \tag{34d}$$

$$\vec{\vec{T}}^{(2)}_{-2} = 1\,\vec{T}^{(1)}_{-1}\vec{T}^{(1)T}_{-1}, \tag{34e}$$

$$\vec{\vec{T}}^{(1)}_{1} = -\frac{1}{\sqrt{2}}\vec{T}^{(1)}_{0}\vec{T}^{(1)T}_{1} + \frac{1}{\sqrt{2}}\vec{T}^{(1)}_{1}\vec{T}^{(1)T}_{0}, \tag{34f}$$

$$\vec{\vec{T}}^{(1)}_{0} = -\frac{1}{\sqrt{2}}T^{(1)}_{-1}\vec{T}^{(1)T}_{1} + \frac{1}{\sqrt{2}}\vec{T}^{(1)}_{1}\vec{T}^{(1)T}_{-1}, \tag{34g}$$

$$\vec{\vec{T}}^{(1)}_{-1} = \frac{1}{\sqrt{2}}\vec{T}^{(1)}_{0}\vec{T}^{(1)T}_{-1} - \frac{1}{\sqrt{2}}\vec{T}^{(1)}_{-1}\vec{T}^{(1)T}_{0}, \tag{34h}$$

$$\vec{\vec{T}}^{(0)}_{0} = \frac{1}{\sqrt{3}}\vec{T}^{(1)}_{-1}\vec{T}^{(1)T}_{1} - \frac{1}{\sqrt{3}}\vec{T}^{(1)}_{0}\vec{T}^{(1)T}_{0} + \frac{1}{\sqrt{3}}\vec{T}^{(1)}_{1}\vec{T}^{(1)T}_{-1}. \tag{34i}$$

As an example of how to perform one of these calculations, we explicitly derive the $\vec{\vec{T}}^{(2)}_{0}$ spherical tensor in equations (35a)–(35d) below:

$$\vec{\vec{T}}^{(2)}_{0} = \frac{1}{\sqrt{6}}\vec{T}^{(1)}_{-1}\vec{T}^{(1)T}_{1} + \frac{2}{\sqrt{6}}\vec{T}^{(1)}_{0}\vec{T}^{(1)T}_{0} + \frac{1}{\sqrt{6}}\vec{T}^{(1)}_{1}\vec{T}^{(1)T}_{-1}, \tag{35a}$$

$$\begin{aligned}\vec{\vec{T}}^{(2)}_{0} = {} & \frac{1}{\sqrt{6}}\begin{pmatrix} \frac{1}{\sqrt{2}} \\ -\frac{i}{\sqrt{2}} \\ 0 \end{pmatrix}\begin{pmatrix} -\frac{1}{\sqrt{2}} & -\frac{i}{\sqrt{2}} & 0 \end{pmatrix} \\ & + \frac{2}{\sqrt{6}}\begin{pmatrix} 0 \\ 0 \\ 1 \end{pmatrix}\begin{pmatrix} 0 & 0 & 1 \end{pmatrix} \\ & + \frac{1}{\sqrt{6}}\begin{pmatrix} -\frac{1}{\sqrt{2}} \\ -\frac{i}{\sqrt{2}} \\ 0 \end{pmatrix}\begin{pmatrix} \frac{1}{\sqrt{2}} & -\frac{i}{\sqrt{2}} & 0 \end{pmatrix},\end{aligned} \tag{35b}$$

$$\overrightarrow{\overrightarrow{T}}_0^{(2)} = \frac{1}{\sqrt{6}}\begin{pmatrix} -\frac{1}{2} & -\frac{i}{2} & 0 \\ \frac{i}{2} & -\frac{1}{2} & 0 \\ 0 & 0 & 0 \end{pmatrix} + \frac{2}{\sqrt{6}}\begin{pmatrix} 0 & 0 & 0 \\ 0 & 0 & 0 \\ 0 & 0 & 1 \end{pmatrix} + \frac{1}{\sqrt{6}}\begin{pmatrix} -\frac{1}{2} & \frac{i}{2} & 0 \\ -\frac{i}{2} & -\frac{1}{2} & 0 \\ 0 & 0 & 0 \end{pmatrix}, \tag{35c}$$

$$\overrightarrow{\overrightarrow{T}}_0^{(2)} = \begin{pmatrix} -\frac{1}{\sqrt{6}} & 0 & 0 \\ 0 & -\frac{1}{\sqrt{6}} & 0 \\ 0 & 0 & \frac{2}{\sqrt{6}} \end{pmatrix}. \tag{35d}$$

All of the other spherical tensors shown in equations (6a)–(6i) can be constructed in an equivalent manner to that shown above (equations (35a)–(35d)).

## 5. The Hamiltonian and Clebsch–Gordan Coefficients

*5.1. The Spherical Components of Hamiltonian.* The Clebsch–Gordan coefficients allow for a quick determination of the terms of the Hamiltonian and how they change upon a rotation. Conveniently, in addition to being able to be used to generate the spherical tensors themselves, they can also be used to generate the spherical components of the Hamiltonian from the corresponding spherical tensor coefficients. This is shown in equations (36a)–(36i) below:

$$\hat{s}_2^{(2)} = 1\left(-\frac{1}{\sqrt{2}}\hat{I}_+\right)\left(-\frac{1}{\sqrt{2}}\hat{S}_+\right) = \frac{1}{2}\hat{I}_+\hat{S}_+, \tag{36a}$$

$$\begin{aligned}\hat{s}_1^{(2)} &= \frac{1}{\sqrt{2}}\left(\hat{I}_z\right)\left(-\frac{1}{\sqrt{2}}\hat{S}_+\right) + \frac{1}{\sqrt{2}}\left(-\frac{1}{\sqrt{2}}\hat{I}_+\right)\left(\hat{S}_z\right) \\ &= -\frac{1}{2}\hat{I}_z\hat{S}_+ - \frac{1}{2}\hat{I}_+\hat{S}_z,\end{aligned} \tag{36b}$$

$$\begin{aligned}\hat{s}_0^{(2)} &= \frac{1}{\sqrt{6}}\left(\frac{1}{\sqrt{2}}\hat{I}_-\right)\left(-\frac{1}{\sqrt{2}}\hat{S}_+\right) + \frac{2}{\sqrt{6}}\left(\hat{I}_z\right)\left(\hat{S}_z\right) + \frac{1}{\sqrt{6}}\left(-\frac{1}{\sqrt{2}}\hat{I}_+\right)\left(\frac{1}{\sqrt{2}}\hat{S}_-\right) \\ &= -\frac{1}{2\sqrt{6}}\hat{I}_-\hat{S}_+ + \frac{2}{\sqrt{6}}\hat{I}_z\hat{S}_z - \frac{1}{2\sqrt{6}}\hat{I}_+\hat{S}_-,\end{aligned} \tag{36c}$$

$$\begin{aligned}\hat{s}_{-1}^{(2)} &= \frac{1}{\sqrt{2}}\left(\hat{I}_z\right)\left(\frac{1}{\sqrt{2}}\hat{S}_-\right) + \frac{1}{\sqrt{2}}\left(\frac{1}{\sqrt{2}}\hat{I}_-\right)\left(\hat{S}_z\right) \\ &= \frac{1}{2}\hat{I}_z\hat{S}_- + \frac{1}{2}\hat{I}_-\hat{S}_z,\end{aligned} \tag{36d}$$

$$\hat{s}_{-2}^{(2)} = 1\left(\frac{1}{\sqrt{2}}\hat{I}_-\right)\left(\frac{1}{\sqrt{2}}\hat{S}_-\right) = \frac{1}{2}\hat{I}_-\hat{S}_-, \tag{36e}$$

$$\begin{aligned}\hat{s}_1^{(1)} &= -\frac{1}{\sqrt{2}}\left(\hat{I}_z\right)\left(-\frac{1}{\sqrt{2}}\hat{S}_+\right) + \frac{1}{\sqrt{2}}\left(-\frac{1}{\sqrt{2}}\hat{I}_+\right)\left(\hat{S}_z\right) \\ &= \frac{1}{2}\hat{I}_z\hat{S}_+ - \frac{1}{2}\hat{I}_+\hat{S}_z,\end{aligned} \tag{36f}$$

$$\begin{aligned}\hat{s}_0^{(1)} &= -\frac{1}{\sqrt{2}}\left(\frac{1}{\sqrt{2}}\hat{I}_-\right)\left(-\frac{1}{\sqrt{2}}\hat{S}_+\right) + \frac{1}{\sqrt{2}}\left(-\frac{1}{\sqrt{2}}\hat{I}_+\right)\left(\frac{1}{\sqrt{2}}\hat{S}_-\right) \\ &= \frac{1}{2\sqrt{2}}\hat{I}_-\hat{S}_+ - \frac{1}{2\sqrt{2}}\hat{I}_+\hat{S}_-,\end{aligned} \tag{36g}$$

$$\begin{aligned}\hat{s}_{-1}^{(1)} &= \frac{1}{\sqrt{2}}\left(\hat{I}_z\right)\left(\frac{1}{\sqrt{2}}\hat{S}_-\right) - \frac{1}{\sqrt{2}}\left(\frac{1}{\sqrt{2}}\hat{I}_-\right)\left(\hat{S}_z\right) \\ &= \frac{1}{2}\hat{I}_z\hat{S}_- - \frac{1}{2}\hat{I}_-\hat{S}_z,\end{aligned} \tag{36h}$$

$$\begin{aligned}\hat{s}_0^{(0)} &= \frac{1}{\sqrt{3}}\left(\frac{1}{\sqrt{2}}\hat{I}_-\right)\left(-\frac{1}{\sqrt{2}}\hat{S}_+\right) - \frac{1}{\sqrt{3}}\left(\hat{I}_z\right)\left(\hat{S}_z\right) + \frac{1}{\sqrt{3}}\left(-\frac{1}{\sqrt{2}}\hat{I}_+\right)\left(\frac{1}{\sqrt{2}}\hat{S}_-\right) \\ &= -\frac{1}{2\sqrt{3}}\hat{I}_-\hat{S}_+ - \frac{1}{\sqrt{3}}\hat{I}_z\hat{S}_z - \frac{1}{2\sqrt{3}}\hat{I}_+\hat{S}_-,\end{aligned} \tag{36i}$$

These are the same $\hat{s}_m^{(l)}$'s that are mentioned in equation (7). In equations (36a)–(36i), the one-spin spherical tensor operators for spin I are $-(1/\sqrt{2})\hat{I}_+$, $\hat{I}_z$, and $(1/\sqrt{2})\hat{I}_-$, for the $m = 1$, $m = 0$, and $m = -1$ cases, respectively. The analogous expressions are used for the S-operators. $\hat{I}_+$ and $\hat{I}_-$ are the raising and lowering operators for spin I (again, analogous quantities exist for the S-operators). Their relationship to the Cartesian operators is shown in equations (37a) and (37b) below:

$$\hat{I}_+ = \hat{I}_x + i\hat{I}_y, \tag{37a}$$

$$\hat{I}_- = \hat{I}_x - i\hat{I}_y. \tag{37b}$$

These expressions can be used to write equations (36a)–(36i) in the manner done in equations (38a)–(38i) below:

$$\hat{s}_2^{(2)} = \frac{1}{2}\hat{I}_x\hat{S}_x - \frac{1}{2}\hat{I}_y\hat{S}_y - \frac{i}{2}\hat{I}_x\hat{S}_y - \frac{i}{2}\hat{I}_y\hat{S}_x, \tag{38a}$$

$$\hat{s}_1^{(2)} = -\frac{1}{2}\hat{I}_z\hat{S}_x - \frac{1}{2}\hat{I}_x\hat{S}_z + \frac{i}{2}\hat{I}_z\hat{S}_y + \frac{i}{2}\hat{I}_y\hat{S}_z, \tag{38b}$$

$$\hat{s}_0^{(2)} = \frac{2}{\sqrt{6}}\hat{I}_z\hat{S}_z - \frac{1}{\sqrt{6}}\hat{I}_x\hat{S}_x - \frac{1}{\sqrt{6}}\hat{I}_y\hat{S}_y, \tag{38c}$$

$$\hat{s}_{-1}^{(2)} = \frac{1}{2}\hat{I}_z\hat{S}_x + \frac{1}{2}\hat{I}_x\hat{S}_z + \frac{i}{2}\hat{I}_z\hat{S}_y + \frac{i}{2}\hat{I}_y\hat{S}_z, \tag{38d}$$

$$\hat{s}_{-2}^{(2)} = \frac{1}{2}\hat{I}_x\hat{S}_x - \frac{1}{2}\hat{I}_y\hat{S}_y + \frac{i}{2}\hat{I}_x\hat{S}_y + \frac{i}{2}\hat{I}_y\hat{S}_x, \tag{38e}$$

$$\hat{s}_1^{(1)} = -\frac{1}{2}\hat{I}_z\hat{S}_x + \frac{1}{2}\hat{I}_x\hat{S}_z + \frac{i}{2}\hat{I}_z\hat{S}_y - \frac{i}{2}\hat{I}_y\hat{S}_z, \tag{38f}$$

$$\hat{s}_0^{(1)} = \frac{i}{\sqrt{2}}\hat{I}_x\hat{S}_y - \frac{i}{\sqrt{2}}\hat{I}_y\hat{S}_x, \tag{38g}$$

$$\hat{s}_{-1}^{(1)} = -\frac{1}{2}\hat{I}_z\hat{S}_x + \frac{1}{2}\hat{I}_x\hat{S}_z - \frac{i}{2}\hat{I}_z\hat{S}_y + \frac{i}{2}\hat{I}_y\hat{S}_z, \tag{38h}$$

$$\hat{s}_0^{(0)} = -\frac{1}{\sqrt{3}}\hat{I}_x\hat{S}_x - \frac{1}{\sqrt{3}}\hat{I}_y\hat{S}_y - \frac{1}{\sqrt{3}}\hat{I}_z\hat{S}_z. \tag{38i}$$

The quantities derived in equations (36a)–(36i) deal with the spin space portion of equations (4) and (7) (the $\hat{s}_m^{(l)}$'s). These are analogous to the terms of the physical space portion of the Hamiltonian (the $a_m^{(l)}$'s) shown in equations (8a)–(8i). Once the spherical components of the Hamiltonian have been determined, equation (30) can be used to quickly transform between various frames of reference, which is useful in the simulation of experiments involving magic angle spinning, for example. A common MAS problem will involve 3 applications of equation (30). First, one will rotate from the principal axis frame of each interaction to a common, crystallite frame (it is often convenient, but not necessary, to choose a crystallite frame that is coincident with the principal axes of one of the interactions). The crystallite frame is then rotated to a frame of reference fixed on the rotor. Finally, a time-dependent transformation is performed from the rotor fixed frame to the lab frame [17]. An example of the results of this type of simulation is shown in Figure 1. In the static case, broad powder patterns are observed for the two resonances pictured. As the rotor begins to spin, the powder patterns break into a manifold of spinning sidebands. Eventually, the rotor spins at a high enough frequency to remove all of the second rank anisotropic interactions and narrow resonances are observed. These simulations were performed using techniques previously described by the authors [26]. Note, however, that MAS does not fully remove many higher-order interactions such as the second-order quadrupole coupling and others that were not included in this simulation [27].

*5.2. Spatial Rotations and the Secular Approximation.* In many magnetic resonance simulations, and in particular those involving spin-1/2 nuclei, it is convenient to make the secular approximation. This process is made straightforward using the spherical tensor operators constructed using Clebsch–Gordan coefficients. This is demonstrated well by the following example involving the static, heteronuclear dipolar coupling interaction. It shows how the convenient properties of the spherical tensor components in both the spin and physical space components of the Hamiltonian

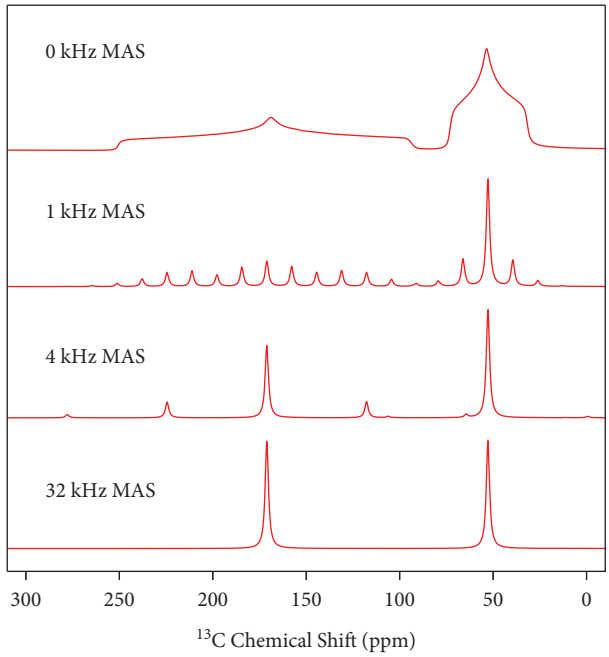


FIGURE 1: Simulations of powder patterns caused by the chemical shift anisotropy interaction at 0, 1, 4, and 32 kHz of MAS. These arise from the time modulation of the interactions present, which can be derived from the spherical tensor operators.

make for a relatively compact way of performing rotations and truncating the Hamiltonian.

*5.2.1. Angular Dependence of Hamiltonian.* Recognizing that the first rank terms of the Hamiltonian are zero (because the physical space coefficients are zero in the principal axis frame, they must be zero in all frames of reference), the Hamiltonian of equation (7) can be written as in equation (39) below:

$$\hat{H} = a_0^{(0)}\hat{s}_0^{(0)} + \sum_{m=-2}^{2} (-1)^m a_m^{(2)}\hat{s}_{-m}^{(2)}. \tag{39}$$

From here, equations (36a)–(36i) can be substituted into equation (39). This substitution is performed in equation (40) below:

$$\begin{aligned}
\hat{H} = {} & a_0^{(0)}\left[-\frac{1}{2\sqrt{3}}\hat{I}_-\hat{S}_+ - \frac{1}{\sqrt{3}}\hat{I}_z\hat{S}_z - \frac{1}{2\sqrt{3}}\hat{I}_+\hat{S}_-\right] \\
& + a_2^{(2)}\left[\frac{1}{2}\hat{I}_-\hat{S}_-\right] \\
& - a_1^{(2)}\left[\frac{1}{2}\hat{I}_z\hat{S}_- + \frac{1}{2}\hat{I}_-\hat{S}_z\right] \\
& + a_0^{(2)}\left[-\frac{1}{2\sqrt{6}}\hat{I}_-\hat{S}_+ + \frac{2}{\sqrt{6}}\hat{I}_z\hat{S}_z - \frac{1}{2\sqrt{6}}\hat{I}_+\hat{S}_-\right] \\
& - a_{-1}^{(2)}\left[-\frac{1}{2}\hat{I}_z\hat{S}_+ - \frac{1}{2}\hat{I}_+\hat{S}_z\right] \\
& + a_{-2}^{(2)}\left[\frac{1}{2}\hat{I}_+\hat{S}_+\right].
\end{aligned} \tag{40}$$

Now, we can evaluate the physical space components. These are given in terms of their Cartesian components in equations (8a)–(8i). However, in practice, the physical space components are characterized in terms of their principal axis values ($a_{XX}$, $a_{YY}$, and $a_{ZZ}$) in the form of three parameters known as the isotropic value ($a_{\text{iso}}$), the anisotropic value ($a_{\text{iso}}$), and the asymmetry parameter ($\eta$). The relationships between these 6 values are given by equations (41a)–(41c). By convention, $a_{XX}$, $a_{YY}$, and $a_{ZZ}$ are identified by the relationship $|a_{ZZ} - a_{\text{iso}}| \geq |a_{XX} - a_{\text{iso}}| \geq |a_{YY} - a_{\text{iso}}|$ [17].

$$a_{\text{iso}} = \frac{1}{3}\left(a_{XX} + a_{YY} + a_{ZZ}\right), \tag{41a}$$

$$a_{\text{aniso}} = a_{ZZ} - a_{\text{iso}}, \tag{41b}$$

$$\eta = \frac{a_{YY} - a_{XX}}{a_{\text{aniso}}}. \tag{41c}$$

Substituting equations (41a)–(41c) into (8a)–(8i), we can write the physical space coefficients in the principal axis frame in terms of $a_{\text{iso}}$, $a_{\text{aniso}}$, and $\eta$. This is shown in equations (42a)–(42i) below [17]:

$$a_2^{(2)}(\text{PAS}) = -\frac{1}{2}\eta a_{\text{aniso}}, \tag{42a}$$

$$a_1^{(2)}(\text{PAS}) = 0, \tag{42b}$$

$$a_0^{(2)}(\text{PAS}) = \frac{\sqrt{6}}{2}a_{\text{aniso}}, \tag{42c}$$

$$a_{-1}^{(2)}(\text{PAS}) = 0, \tag{42d}$$

$$a_{-2}^{(2)}(\text{PAS}) = -\frac{1}{2}\eta a_{\text{aniso}}, \tag{42e}$$

$$a_1^{(1)}(\text{PAS}) = 0, \tag{42f}$$

$$a_0^{(1)}(\text{PAS}) = 0, \tag{42g}$$

$$a_{-1}^{(1)}(\text{PAS}) = 0, \tag{42h}$$

$$a_0^{(0)}(\text{PAS}) = -\sqrt{3}a_{\text{iso}}. \tag{42i}$$

For the dipolar coupling interaction, $a_{iso} = 0$, $a_{\text{aniso}} = 2\omega_D$, and $\eta = 0$. Thus, only $a_0^{(2)}(\text{PAS})$ is nonzero. We know what $a_0^{(2)}(\text{PAS})$ is, but we want $a_0^{(2)}$ in the lab frame. This can be evaluated by using a property of the spherical components that makes such transformations straightforward. This is shown in equation (43) below [17]:

$$a_m^{(l)}(\text{new frame}) = \sum_{m=-l}^{l} D_{m,m'}^{(l)}\left(\Omega_{\text{PAS}}^{\text{lab}}\right)a_{m'}^{(l)}(\text{old frame}). \tag{43}$$

Here, the $D_{m,m'}^{(l)}(\Omega_{\text{PAS}}^{\text{lab}})$'s are the Wigner rotation matrix elements and are readily available in the literature [17].

Equation (43) is the component analog of the tensor rotation equation in equation (30). $\Omega_{\mathrm{PAS}}^{\mathrm{lab}}$ is the set of $\alpha, \beta$, and $\gamma$ Euler angles that describe the rotation from the principal axis frame to the lab frame. Because $a_0^{(2)}(\mathrm{PAS})$ is the only nonzero principal axis frame component, its value in the lab frame can be written as is shown in equation (44) below [17]:

$$a_0^{(2)} = D_{0,0}^{(2)}\left(\Omega_{\mathrm{PAS}}^{\mathrm{lab}}\right) a_0^{(2)}(\mathrm{PAS}). \tag{44}$$

We can now make the substitution $D_{0,0}^{(2)}(\Omega_{\mathrm{PAS}}^{lab}) = (1/2)(3\cos^2(\beta_{\mathrm{PAS}}^{\mathrm{lab}}) - 1)$. This is shown in equation (45). We have also substituted in equations (42c) and (44) for $a_0^{(2)}(\mathrm{PAS})$.

$$a_0^{(2)} = \frac{1}{2}\left(3\cos^2\left(\beta_{\mathrm{PAS}}^{\mathrm{lab}}\right) - 1\right)(2)\left(\frac{\sqrt{6}}{2}\right)\omega_D. \tag{45}$$

The expression in equation (45) is rewritten in the form of equation (46) below:

$$a_0^{(2)} = \frac{\sqrt{6}}{2}\omega_D\left(3\cos^2\left(\beta_{\mathrm{PAS}}^{\mathrm{lab}}\right) - 1\right). \tag{46}$$

Substituting equation (46) into equation (40) yields equation (47):

$$\hat{H} = \frac{\sqrt{6}}{2}\omega_D\left(3\cos^2\left(\beta_{\mathrm{PAS}}^{\mathrm{lab}}\right) - 1\right) \left[-\frac{1}{2\sqrt{6}}\hat{I}_-\hat{S}_+ + \frac{2}{\sqrt{6}}\hat{I}_z\hat{S}_z - \frac{1}{2\sqrt{6}}\hat{I}_+\hat{S}_-\right]. \tag{47}$$

*5.2.2. The Secular Approximation.* Up until this point, we have used the spherical components of the physical space portion of the Hamiltonian to transform between the principal axis frame and the lab frame. We can also use the spherical components in the spin space portion of the Hamiltonian to conveniently transform into a rotating frame with each spin. This is performed in equation (48) using the unitary operator $\hat{U} = \exp[i\omega_I t\hat{I}_z]\exp[i\omega_S t\hat{S}_z]$, where $\omega_I$ and $\omega_S$ are the Larmor frequencies for the I and S-spins, respectively:

$$\hat{H}_{\mathrm{rot}} = \frac{\sqrt{6}}{2}\omega_D\left(3\cos^2\left(\beta_{\mathrm{PAS}}^{\mathrm{lab}}\right) - 1\right)\hat{U} \left[-\frac{1}{2\sqrt{6}}\hat{I}_-\hat{S}_+ + \frac{2}{\sqrt{6}}\hat{I}_z\hat{S}_z - \frac{1}{2\sqrt{6}}\hat{I}_+\hat{S}_-\right]\hat{U}^{-1}. \tag{48}$$

Recall from equations (36a)–(36i) that $\hat{I}_+$, $\hat{I}_z$, and $\hat{I}_-$, along with the corresponding S-spin operators, are related to the vector spherical tensor operator components. The I-spin operators have the convenient rotational properties shown in equations (49a)–(49c) below, with corresponding relationships for the S-spin operators [28]:

$$\hat{U}\left(-\frac{1}{\sqrt{2}}\hat{I}_+\right)\hat{U}^{-1} = \exp[i\omega_I t]\left(-\frac{1}{\sqrt{2}}\hat{I}_+\right), \tag{49a}$$

$$\hat{U}\left(\frac{1}{\sqrt{2}}\hat{I}_-\right)\hat{U}^{-1} = \exp[-i\omega_I t]\left(\frac{1}{\sqrt{2}}\hat{I}_-\right), \tag{49b}$$

$$\hat{U}\hat{I}_z\hat{U}^{-1} = \hat{I}_z. \tag{49c}$$

Substituting the expressions in equations (49a)–(49c) into equation (48) yields equation (50) below [28]:

$$\hat{H}_{\mathrm{rot}} = \frac{\sqrt{6}}{2}\omega_D\left(3\cos^2\left(\beta_{\mathrm{PAS}}^{\mathrm{lab}}\right) - 1\right) \times\left[-\frac{1}{2\sqrt{6}}\exp[-i(\omega_I - \omega_S)t]\hat{I}_-\hat{S}_+ + \frac{2}{\sqrt{6}}\hat{I}_z\hat{S}_z - \frac{1}{2\sqrt{6}}\exp[i(\omega_I - \omega_S)t]\hat{I}_+\hat{S}_-\right]. \tag{50}$$

Application of first-order average Hamiltonian theory allows equation (50) to be averaged over one period of the frequency $\omega_I - \omega_S$, so long as $|(\omega_I - \omega_S)|$ is much greater than any other interaction in the Hamiltonian. The time-dependent portions average to 0. This is the so-called "secular approximation" and can lead to great simplification of the Hamiltonian and decrease in simulation times. The final, rotating frame secular Hamiltonian is shown in equation (51) below [23]:

$$\overline{\hat{H}}_{\mathrm{rot}} = \omega_D\left(3\cos^2\left(\beta_{\mathrm{PAS}}^{\mathrm{lab}}\right) - 1\right)\hat{I}_z\hat{S}_z. \tag{51}$$

## 6. The Singlet-Triplet Basis

Another common set of Clebsch–Gordan coefficients that arise in magnetic resonance are those of what is referred to as the singlet-triplet basis. This arises from the interaction of two spin-1/2 particles. We can again follow the procedure prescribed in Section 3. First, we need to identify the allowed values of $J$. There are two spin-1/2 particles, so the allowed values of $J$ are $|1/2 - 1/2| \le J \le 1/2 + 1/2$ or $0 \le J \le 1$. Again, this was adapted from the procedure mentioned in Griffiths [18] and Shankar [21].

We first need to determine the effect of the lowering operators for spin-1/2 and spin-1 on the basis states (the spin-0 state cannot be lowered any further). This is given in Tables 3 and 4.

From here, we determine what the system states are in terms of the states of the component spins. We begin with the state $|j_1, j_2, J, M\rangle = |1/2, 1/2, 1, 1\rangle$ in equation (52) below:

$$\left|\frac{1}{2},\frac{1}{2},1,1\right\rangle = 1\left(\left|\frac{1}{2},\frac{1}{2}\right\rangle \otimes \left|\frac{1}{2},\frac{1}{2}\right\rangle\right). \tag{52}$$

From here, we apply the total lowering operator to obtain $|j_1, j_2, J, M\rangle = |1/2, 1/2, 1, 0\rangle$, as given in equations (53a)–(53c) below:

Table 3: The effect of the spin-1/2 lowering operator on each allowed spin state.

| $j$ | $m$ | $j(j+1)$ | $m(m-1)$ | $j(j+1)-m(m-1)$ | $\sqrt{j(j+1)-m(m-1)}$ |
|---|---|---|---|---|---|
| 1/2 | 1/2 | 3/4 | −1/4 | 1 | 1 |
| 1/2 | −1/2 | 3/4 | 3/4 | 0 | 0 |

Table 4: The effect of the spin-1 lowering operator on each allowed spin state.

| $j$ | $m$ | $j(j+1)$ | $m(m-1)$ | $j(j+1)-m(m-1)$ | $\sqrt{j(j+1)-m(m-1)}$ |
|---|---|---|---|---|---|
| 1 | 1 | 2 | 0 | 2 | $\sqrt{2}$ |
| 1 | 0 | 2 | 0 | 2 | $\sqrt{2}$ |
| 1 | −1 | 2 | 2 | 0 | 0 |

$$\hat{J}_-(1)\left|\frac{1}{2},\frac{1}{2},1,1\right\rangle = \left(\hat{j}_-^{(1)}\left(\frac{1}{2}\right)+\hat{j}_-^{(2)}\left(\frac{1}{2}\right)\right)\left(\left|\frac{1}{2},\frac{1}{2}\right\rangle\otimes\left|\frac{1}{2},\frac{1}{2}\right\rangle\right), \tag{53a}$$

$$\sqrt{2}\left|\frac{1}{2},\frac{1}{2},1,0\right\rangle = \left(\left|\frac{1}{2},-\frac{1}{2}\right\rangle\otimes\left|\frac{1}{2},\frac{1}{2}\right\rangle\right)+\left(\left|\frac{1}{2},\frac{1}{2}\right\rangle\otimes\left|\frac{1}{2},-\frac{1}{2}\right\rangle\right), \tag{53b}$$

$$\left|\frac{1}{2},\frac{1}{2},1,0\right\rangle = \frac{1}{\sqrt{2}}\left(\left|\frac{1}{2},-\frac{1}{2}\right\rangle\otimes\left|\frac{1}{2},\frac{1}{2}\right\rangle\right)+\frac{1}{\sqrt{2}}\left(\left|\frac{1}{2},\frac{1}{2}\right\rangle\otimes\left|\frac{1}{2},-\frac{1}{2}\right\rangle\right). \tag{53c}$$

A subsequent application of the lowering operator yields equations (54a)–(54e) below:

$$\begin{aligned}\hat{J}_-(1)\left|\frac{1}{2},\frac{1}{2},1,0\right\rangle &= \left(\hat{j}_-^{(1)}\left(\frac{1}{2}\right)+\hat{j}_-^{(2)}\left(\frac{1}{2}\right)\right)\\ &\cdot\left(\frac{1}{\sqrt{2}}\left(\left|\frac{1}{2},-\frac{1}{2}\right\rangle\otimes\left|\frac{1}{2},\frac{1}{2}\right\rangle\right)\right.\\ &\left.+\frac{1}{\sqrt{2}}\left(\left|\frac{1}{2},\frac{1}{2}\right\rangle\otimes\left|\frac{1}{2},-\frac{1}{2}\right\rangle\right)\right),\end{aligned} \tag{54a}$$

$$\begin{aligned}\sqrt{2}\left|\frac{1}{2},\frac{1}{2},1,-1\right\rangle &= \frac{1}{\sqrt{2}}\left(\left|\frac{1}{2},-\frac{1}{2}\right\rangle\otimes\left|\frac{1}{2},-\frac{1}{2}\right\rangle\right)\\ &+\frac{1}{\sqrt{2}}\left(\left|\frac{1}{2},-\frac{1}{2}\right\rangle\otimes\left|\frac{1}{2},-\frac{1}{2}\right\rangle\right),\end{aligned} \tag{54b}$$

$$\sqrt{2}\left|\frac{1}{2},\frac{1}{2},1,-1\right\rangle = \frac{2}{\sqrt{2}}\left(\left|\frac{1}{2},-\frac{1}{2}\right\rangle\otimes\left|\frac{1}{2},-\frac{1}{2}\right\rangle\right), \tag{54c}$$

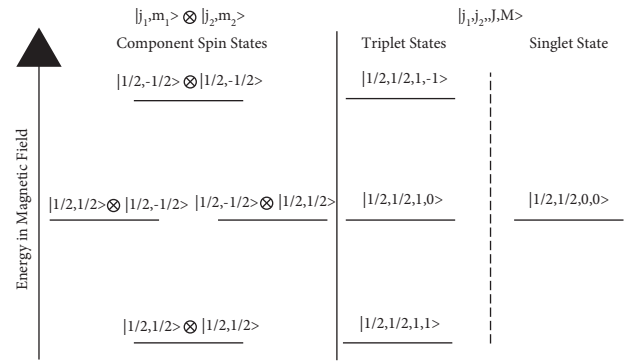


Figure 2: The spin states of a system of two spin-1/2 particles with positive gyromagnetic ratios. The component spin states are depicted on the left and the system spin states on the right.

$$\left|\frac{1}{2},\frac{1}{2},1,-1\right\rangle = \frac{2}{2}\left(\left|\frac{1}{2},-\frac{1}{2}\right\rangle\otimes\left|\frac{1}{2},-\frac{1}{2}\right\rangle\right), \tag{54d}$$

$$\left|\frac{1}{2},\frac{1}{2},1,-1\right\rangle = 1\left(\left|\frac{1}{2},-\frac{1}{2}\right\rangle\otimes\left|\frac{1}{2},-\frac{1}{2}\right\rangle\right). \tag{54e}$$

This completes the three $J = 1$ states (the triplet). We now need to determine what the single $J = 0$ state is (the singlet). This is accomplished by using the orthogonality condition for the basis states, in the same manner that we determined the $|j_1, j_2, J, M\rangle = |1, 1, 1, 1\rangle$ state in Section 3. This is accomplished in equations (55a)–(55f) below:

$$\begin{aligned}\left\langle\frac{1}{2},\frac{1}{2},1,0\middle|\frac{1}{2},\frac{1}{2},0,0\right\rangle &= \left(\frac{1}{\sqrt{2}}\left(\left\langle\frac{1}{2},-\frac{1}{2}\right|\otimes\left\langle\frac{1}{2},\frac{1}{2}\right|\right)+\frac{1}{\sqrt{2}}\left(\left\langle\frac{1}{2},\frac{1}{2}\right|\otimes\left\langle\frac{1}{2},-\frac{1}{2}\right|\right)\right)\\ &\times\left(C^{(1/2,1/2,0)}_{-1/2,1/2,0}\left(\left|\frac{1}{2},-\frac{1}{2}\right\rangle\otimes\left|\frac{1}{2},\frac{1}{2}\right\rangle\right)+C^{(1/2,1/2,0)}_{1/2,-1/2,0}\left(\left|\frac{1}{2},\frac{1}{2}\right\rangle\otimes\left|\frac{1}{2},-\frac{1}{2}\right\rangle\right)\right),\end{aligned} \tag{55a}$$

$$0 = \frac{1}{\sqrt{2}}C^{(1/2,1/2,0)}_{-1/2,1/2,0}+\frac{1}{\sqrt{2}}C^{(1/2,1/2,0)}_{1/2,-1/2,0}, \tag{55b}$$

$$C^{(1/2,1/2,0)}_{-1/2,1/2,0} = -C^{(1/2,1/2,0)}_{1/2,-1/2,0}, \tag{55c}$$

$$C^{(1/2,1/2,0)}_{1/2,-1/2,0} = \frac{1}{\sqrt{2}}, \tag{55d}$$

$$C^{(1/2,1/2,0)}_{-1/2,1/2,0} = -\frac{1}{\sqrt{2}}, \tag{55e}$$

$$\left|\frac{1}{2},\frac{1}{2},0,0\right\rangle = -\frac{1}{\sqrt{2}}\left(\left|\frac{1}{2},-\frac{1}{2}\right\rangle \otimes \left|\frac{1}{2},\frac{1}{2}\right\rangle\right) + \frac{1}{\sqrt{2}}\left(\left|\frac{1}{2},\frac{1}{2}\right\rangle \otimes \left|\frac{1}{2},-\frac{1}{2}\right\rangle\right). \tag{55f}$$

Again, in equations (55d)–(55f), we have used the normalization condition and the Condon–Shortley phase convention to obtain these specific values for the Clebsch–Gordan coefficients. The spin states of the singlet-triplet basis are summarized in equations (56a)–(56d) below:

$$\left|\frac{1}{2},\frac{1}{2},1,1\right\rangle = 1\left(\left|\frac{1}{2},\frac{1}{2}\right\rangle \otimes \left|\frac{1}{2},\frac{1}{2}\right\rangle\right), \tag{56a}$$

$$\left|\frac{1}{2},\frac{1}{2},1,0\right\rangle = \frac{1}{\sqrt{2}}\left(\left|\frac{1}{2},-\frac{1}{2}\right\rangle \otimes \left|\frac{1}{2},\frac{1}{2}\right\rangle\right) + \frac{1}{\sqrt{2}}\left(\left|\frac{1}{2},\frac{1}{2}\right\rangle \otimes \left|\frac{1}{2},-\frac{1}{2}\right\rangle\right), \tag{56b}$$

$$\left|\frac{1}{2},\frac{1}{2},1,-1\right\rangle = 1\left(\left|\frac{1}{2},-\frac{1}{2}\right\rangle \otimes \left|\frac{1}{2},-\frac{1}{2}\right\rangle\right), \tag{56c}$$

$$\left|\frac{1}{2},\frac{1}{2},0,0\right\rangle = -\frac{1}{\sqrt{2}}\left(\left|\frac{1}{2},-\frac{1}{2}\right\rangle \otimes \left|\frac{1}{2},\frac{1}{2}\right\rangle\right) + \frac{1}{\sqrt{2}}\left(\left|\frac{1}{2},\frac{1}{2}\right\rangle \otimes \left|\frac{1}{2},-\frac{1}{2}\right\rangle\right). \tag{56d}$$

An energy level diagram for the spin states shown in equations (56a)–(56d) when they are placed in a magnetic field is shown in Figure 2.

The example described above was for a system of two identical spin-1/2 particles, but higher spin systems can be treated in a similar manner. For example, this could be the 3-electron system of an $N@C_{60}$ endofullerene [29, 30] or the 7-electron DOTA-$Gd^{3+}$ complex [31]. The effects of the lowering operator for all spins between 1/2 and 4 is given in Sections S1–S8 of the Supplementary Materials, respectively.

## 7. Conclusion

The Clebsch–Gordan coefficients play an important part in magnetic resonance simulations. Not only do they allow for higher-order spherical tensors to be constructed from lower order ones but also allow for the spin states of a system to be determined from component spin wave functions in the system. Despite the number of roles that they play in magnetic resonance simulations, an explanation of the origin of the Clebsch–Gordan coefficients is rarely provided, particularly in magnetic resonance literature. Here, we have derived the Clebsch–Gordan coefficients for two tensors of rank 1 to form resultant rank 0, 1, and 2 tensors, determined the angular dependence and secular portion of the static, dipolar coupling Hamiltonian, and derived the triplet and singlet states of two identical spin-1/2 spins. Other uses include determining the spin states of high spin transition metal complexes such as those involving $Gd^{3+}$ [31] and endofullerenes [29, 30] (such as $N@C_{60}$) and for the calculation of the fourth rank tensor components of second-order average Hamiltonians, such as those present in systems with large quadrupolar couplings [32], hyperfine couplings [33], and zero field splittings [34].

## Data Availability

This is an educational article and contains no experimental data.

## Conflicts of Interest

The authors declare that they have no conflicts of interest.

## Acknowledgments

The authors would like to thank Nicholas Alaniva and Sarah A. Overall for checking the work performed here, as well as Thomas O. Popp, Salima Bahri, Natalie Golota, and Ravi Shankar Palani are thanked for useful discussions. Internal funding was provided from the Eidgenössische Technische Hochschule Zürich.

## Supplementary Materials

The supplementary material contains tables calculating the effect of the lowering operator on each $z$ projection state for all spins between 1/2 and 4 as well as a justification for the rule decribed in equation (12b). (*Supplementary Materials*)

## References


[1] A. J. Rossini, C. M. Widdifield, A. Zagdoun et al., "Dynamic nuclear polarization enhanced NMR spectroscopy for pharmaceutical formulations," *Journal of the American Chemical Society*, vol. 136, no. 6, pp. 2324–2334, 2014.

[2] S. Hayes, L. van Wüllen, H. Eckert, W. R. Even, R. W. Crocker, and Z. Zhang, "Solid-state NMR strategies for the structural investigation of carbon-based anode materials," *Chemistry of Materials*, vol. 9, no. 4, pp. 901–911, 1997.

[3] L. A. Baker, T. Sinnige, P. Schellenberger et al., "Combined 1H-detected solid-state NMR spectroscopy and electron cryotomography to study membrane proteins across resolutions in native environments," *Structure*, vol. 26, no. 1, pp. 161.e3–170.e3, 2018.

[4] M. L. Mak-Jurkauskas, V. S. Bajaj, M. K. Hornstein, M. Belenky, R. G. Griffin, and J. Herzfeld, "Energy transformations early in the bacteriorhodopsin photocycle revealed by DNP-enhanced solid-state NMR," *Proceedings of the National Academy of Sciences*, vol. 105, no. 3, pp. 883–888, 2008.

[5] H. Yang, D. Staveness, S. M. Ryckbosch et al., "REDOR NMR reveals multiple conformers for a protein kinase c ligand in a membrane environment," *ACS Central Science*, vol. 4, no. 1, pp. 89–96, 2018.

[6] S. Penzel, A. Oss, M. L. Org et al., "Spinning faster: protein NMR at MAS frequencies up to 126 kHz," *Journal of Biomolecular NMR*, vol. 73, no. 1-2, pp. 19–29, 2019.

[7] R. Rizzato and M. Bennati, "Cross-polarization electron-nuclear double resonance spectroscopy," *ChemPhysChem*, vol. 16, no. 18, pp. 3769–3773, 2015.

[8] N. Alaniva, E. P. Saliba, E. L. Sesti, P. T. Judge, and A. B. Barnes, "Electron decoupling with chirped microwave pulses for rapid signal acquisition and electron saturation recovery," *Angewandte Chemie*, vol. 131, no. 22, 2019.

[9] E. P. Saliba, E. L. Sesti, N. Alaniva, and A. B. Barnes, "Pulsed electron decoupling and strategies for time domain dynamic nuclear polarization with magic angle spinning," *The Journal of Physical Chemistry Letters*, vol. 9, no. 18, pp. 5539–5547, 2018.

[10] E. P. Saliba, E. L. Sesti, F. J. Scott et al., "Electron decoupling with dynamic nuclear polarization in rotating solids," *Journal of the American Chemical Society*, vol. 139, no. 18, pp. 6310–6313, 2017.

[11] E. L. Sesti, E. P. Saliba, N. Alaniva, and A. B. Barnes, "Electron decoupling with cross polarization and dynamic nuclear polarization below 6 K," *Journal of Magnetic Resonance*, vol. 295, pp. 1–5, 2018.

[12] L. R. Becerra, G. J. Gerfen, R. J. Temkin, D. J. Singel, and R. G. Griffin, "Dynamic nuclear polarization with a cyclotron resonance maser at 5 T," *Physical Review Letters*, vol. 71, no. 21, pp. 3561–3564, 1993.

[13] S. A. Overall, J. S. Toor, S. Hao et al., "High throughput pMHC-I tetramer library production using chaperone mediated peptide exchange," *Nature Communications*, vol. 11, no. 1, 2020.

[14] S. D. Cady, K. Schmidt-Rohr, J. Wang, C. S. Soto, W. F. DeGrado, and M. Hong, "Structure of the amantadine binding site of influenza M2 proton channels in lipid bilayers," *Nature*, vol. 463, no. 7281, pp. 689–692, 2010.

[15] T. M. Osborn Popp, J. B. Addison, J. S. Jordan et al., "Surface and wetting properties of embiopteran (webspinner) nanofiber silk," *Langmuir*, vol. 32, no. 18, pp. 4681–4687, 2016.

[16] L. Delage-laurin, R. S. Palani, N. Golota, M. Mardini, Y. Ouyang, and K. O. Tan, "Overhauser dynamic nuclear polarization with selectively deuterated BDPA radicals," *Journal of the American Chemical Society*, vol. 143, no. 48, 2021.

[17] L. J. Mueller, "Tensors and rotations in NMR," *Concepts in Magnetic Resonance: Part A*, vol. 38A, no. 5, pp. 221–235, 2011.

[18] D. J. Griffiths, *Introduction to Quantum Mechanics*, Pearson Education, London, UK, 2nd edition, 2005.

[19] M. Mehring and V. A. Weberuss, *Object-Oriented Magnetic Resonance: Classes and Objects, Calculations and Computations*, Academic Press, Cambridge, MA, USA, 2001.

[20] S. D. Majumdar, "The clebsch-gordan coefficients," *Progress of Theoretical Physics*, vol. 20, no. 6, pp. 798–803, 1958.

[21] R. Shankar, *Principles of Quantum Mechanics*, Springer Science+Business Media, LLC, Berlin, Germany, 2nd edition, 1994.

[22] C. Cohen-Tannoudji, B. Diu, and F. Laloë, *Quantum mechanics*, vol. 2, Wiley, New York, NY, USA, 1977.

[23] M. H. Levitt, *Spin Dynamics*, John Wiley & Sons Ltd., Hoboken, NJ, USA, 2nd edition, 2008.

[24] G. E. Baird and L. C. Biedenharn, "On the representations of the semisimple lie groups. III. the explicit conjugation operation for SUn," *Journal of Mathematical Physics*, vol. 5, no. 12, pp. 1723–1730, 1964.

[25] S. Wolfram, *The Mathematica Book*, Assembly Automation, Duarte, CA, USA, 3rd edition, 1999.

[26] E. P. Saliba and A. B. Barnes, "Fast electron paramagnetic resonance magic angle spinning simulations using analytical powder averaging techniques," *The Journal of Chemical Physics*, vol. 151, no. 11, Article ID 114107, 2019.

[27] T. M. Osborn Popp, N. H. Alaniva, and A. B. Barnes, "Setting the magic angle using single crystal sapphire rotors," *Journal of Magnetic Resonance Open*, vol. 8-9, no. 9, Article ID 100019, 2021.

[28] M. Edén, "Zeeman truncation in NMR. II. Time averaging in the rotating frame," *Concepts in Magnetic Resonance: Part A*, vol. 43, no. 4, pp. 109–126, 2014.

[29] C. Meyer, W. Harneit, B. Naydenov, K. Lips, and A. Weidinger, "N@C60 and P@C60 as quantum bits," *Applied Magnetic Resonance*, vol. 27, no. 1-2, pp. 123–132, 2004.

[30] J. J. Wittmann, T. V. Can, M. Eckardt, W. Harneit, R. G. Griffin, and B. Corzilius, "High-precision measurement of the electron spin g factor of trapped atomic nitrogen in the endohedral fullerene N@C60," *Journal of Magnetic Resonance*, vol. 290, pp. 12–17, 2018.

[31] M. Kaushik, M. Qi, A. Godt, and B. Corzilius, "Bis-gadolinium complexes for solid effect and cross effect dynamic nuclear polarization," *Angewandte Chemie International Edition*, vol. 56, no. 15, pp. 4295–4299, 2017.

[32] P. P. Man, "Quadrupole couplings in nuclear magnetic resonance," *General. Encyclopedia of Analytical Chemistry*, pp. 12224–12265, John Wiley & Sons Ltd, Chichester, UK, 2006.

[33] B. Corzilius, "Theory of solid effect and cross effect dynamic nuclear polarization with half-integer high-spin metal polarizing agents in rotating solids," *Physical Chemistry Chemical Physics*, vol. 18, no. 39, pp. 27190–27204, 2016.

[34] M. Benmelouka, A. Borel, L. Moriggi, L. Helm, and A. E. Merbach, "Design of Gd(III)-based magnetic resonance imaging contrast agents: static and transient zero-field splitting contributions to the electronic relaxation and their impact on relaxivity," *The Journal of Physical Chemistry B*, vol. 111, no. 4, pp. 832–840, 2007.